Author's pre-print of a Chapter accepted to *AGU Monograph:*
Crustal Magmatic System Evolution: Anatomy, Architecture and Physico-Chemical Processes
Eds. Masotta, M., Beier, C. & Mollo S., ISBN: 9781119564454, Wiley

From Binary Mixing to Magma Chamber Simulator – Geochemical Modeling of Assimilation in Magmatic Systems

Jussi S. Heinonen[1], Kieran A. Iles[1,2], Aku Heinonen[1], Riikka Fred[1], Ville J. Virtanen[1], Wendy A. Bohrson[3,4], and Frank J. Spera[5]

[1] Department of Geosciences and Geography, P.O. Box 64, University of Helsinki, 00014, Helsinki, Finland
[2] Present address: Finnish Museum of Natural History, P.O. Box 44, University of Helsinki, 00014, Helsinki, Finland
[3] Department of Geological Sciences, Central Washington University, 400 E University Way, Ellensburg, WA 98926, USA
[4] Present address: Geology and Geological Engineering Department, Colorado School of Mines, 1516 Illinois St., Golden, CO 80401, USA
[5] Department of Earth Science and Earth Research Institute, University of California Santa Barbara, Lagoon Rd, Santa Barbara, CA 93106, USA

Corresponding author: Jussi S. Heinonen (jussi.s.heinonen@helsinki.fi)

Key points (max 140 characters each)

- Assimilation is conceptually defined as an end-member mode of magmatic interaction
- Geochemical models of assimilation are reviewed and discussed
- Assimilation can have notable effects on the geochemical signatures of magmatic systems

Abstract

Magmas readily react with their surroundings, which may be other magmas or solid rocks. Such reactions are important in the chemical and physical evolution of magmatic systems and the crust, for example, in inducing volcanic eruptions and in the formation of ore deposits. In this contribution, we conceptually distinguish assimilation from other modes of magmatic interaction and discuss and review a range of geochemical (± thermodynamical) models used to model assimilation. We define *assimilation* in its simplest form as an end-member mode of magmatic interaction in which an initial state (t_0) that includes a system of melt and solid wallrock evolves to a later state (t_n) where the two entities have been homogenized. In complex natural systems, assimilation can refer more broadly to a process where a mass of magma wholly or partially homogenizes with materials derived from wallrock that initially behaves as a solid. The first geochemical models of assimilation used binary mixing equations and then evolved to incorporate mass balance between a constant-composition assimilant and magma undergoing simultaneous fractional crystallization. More recent tools incorporate energy and mass conservation in order to simulate changing magma composition as wallrock undergoes partial melting. For example, the Magma Chamber Simulator utilizes thermodynamic constraints to document the phase equilibria and major element, trace element, and isotopic evolution of an assimilating and crystallizing magma body. Such thermodynamic considerations are prerequisite for understanding the importance and thermochemical consequences of assimilation in nature, and confirm that bulk assimilation of large amounts of solid wallrock is limited by the enthalpy available from the crystallizing resident magma. Nevertheless, the geochemical signatures of magmatic systems – although dominated for

some elements (particularly major elements) by crystallization processes – may be influenced by simultaneous assimilation of partial melts of compositionally distinct wallrock.

Keywords: geochemistry, assimilation, modeling, magma, mixing

1 Introduction

Before Bowen (1915a, 1915b, 1915c, 1928) demonstrated the significance of fractional crystallization, assimilation of country (wall-) rocks and mixing of magmas (Bunsen, 1851) were considered the primary means leading to the diversity of magma compositions and hence igneous rocks (e.g., Daly, 1905, 1910; Fenner, 1926; see McBirney, 1979). During Bowen's time, there were few petrologists able to utilize experimental methods, and thermodynamic properties of silicate phases were too poorly constrained to quantitatively investigate the physico-chemical consequences of assimilation. The initial assessment of the assimilation hypothesis was largely based on rudimentary major element data and field observations (e.g., often diffuse or stoped contact zones at the intrusion-wallrock interface). Bowen's initial findings, its ripples over the decades, and the accumulation of evidence from experimental petrology have shown that formation of large amounts of country rock melt is limited by the enthalpy available from the magma (e.g., Bowen, 1928; Wilcox, 1954; Pushkar et al., 1971; McBirney, 1979; Taylor, 1980; Nicholls & Stout, 1982; Sparks, 1986; Reiners et al., 1995). Furthermore, the heat required to melt wallrock cannot come from the sensible heat of the magma alone, but also requires a substantial amount of heat released by its crystallization (i.e., latent heat of crystallization).

Regardless of crystallization being recognized as the single most effective process in modifying major element compositions of magmas (Bowen, 1928), simultaneous assimilation is possible and has been described in many geological environments. Assimilation of compositionally distinct country rocks has been shown to have a considerable effect on the trace element and isotopic compositions of crystallizing magmas (e.g., Carter et al., 1978; Taylor, 1980; Huppert et al., 1985; Hansen & Nielsen, 1999; Tegner et al., 1999; Bohrson & Spera, 2001; Heinonen et al., 2016). Identifying mantle sources of basalts in different environments relies heavily on constraining the effects of crustal assimilation (e.g., Carlson, 1991; Lightfoot et al., 1993; Ramos & Reid, 2005; Jung et al., 2011; Borisova et al., 2017). Assimilation may also be important in formation of economically valuable mineralizations: for example, in some magmatic Ni-Cu-PGE sulfide deposits, a large portion of S is thought to be derived from assimilated sedimentary country rocks (e.g., Mariga et al., 2006; Thakurta et al., 2008; Hayes et al., 2015; Iacono-Marziano et al., 2017; Samalens et al., 2017). In addition, assimilation processes influence the eruptive behavior of many volcanic systems, especially by increasing the volatile budgets of magmas (e.g., Borisova et al., 2013; Gardner et al., 2013; Handley et al., 2018).

Before venturing further, we seek to clarify what the term *assimilation* means with respect to magmatic systems. How does "assimilation" differ from "mixing"? Some of the earliest chemical models of assimilation actually used a simple binary mixing equation. Geoscientists have subsequently had difficulties agreeing on a consistent lexicon for assimilation phenomena. For example, in the 1st edition of the Glossary of Geology (Gary et al., 1972; p. 42), assimilation is described as: "The process of incorporating solid or fluid foreign material, i.e., wallrock, into magma. The term implies no specific mechanisms or results. Such a magma, or the rock it produces,

may be called *hybrid* or *anomalous*." More than 30 years later in the 5th edition (Neuendorf et al., 2005; p. 40), the description had evolved to: "The incorporation and digestion of xenoliths and their chemical constituents into a body of magma. Such a magma, or the rock it produces, may be called *hybrid* or *contaminated*." These murky definitions create confusion, and consequently, the first part of this contribution concentrates on distinguishing end-member modes of magmatic interaction: hybridization (complete chemical mixing of two melts) versus mingling (the mixed melts stay separated chemically) versus assimilation (complete chemical mixing of a melt and its initially solid wallrock) versus stoping (the melt and wallrock blocks stay separated chemically). The outcomes of these pure end-member modes can all be considered mixtures – either homogeneous (mixing and assimilation) or heterogeneous (mingling and stoping). We do the division by constraining the initial (t_0) and later (t_n) states of the system for each end-member interaction mode. By establishing this framework, intermediate forms of interaction that are of geological interest can be placed in relation to these end-member modes and the mathematical models that describe them.

The second part of this chapter reviews the development of geochemical modeling of assimilation: how models evolved from a binary mixing equation (e.g., Bell & Powell, 1969; Faure et al., 1974; Vollmer, 1976) through more complicated but still purely chemical models, such as the widely used assimilation fractional-crystallization (AFC) model of DePaolo (1981; hereafter referred to as AFC_{DP}; see also O'Hara, 1977; Allégre & Minster, 1978; Taylor, 1980), towards energy-constrained AFC (EC-AFC) models that take into account the heat budget of the system (Bohrson & Spera, 2001, 2003, 2007; Spera & Bohrson, 2001, 2002, 2004). The energy-constrained approach has most recently culminated in the development of the Magma Chamber Simulator (MCS; Bohrson et al., 2014, 2020; Heinonen et al., 2020) that also considers phase equilibria. Here, we provide a comprehensive historical overview of the concepts associated with the modeling of assimilation. We review usefulness of the different geochemical models of assimilation in magmatic systems and provide an example of MCS applied to a natural system (continental flood basalts).

2 The end-member modes of magmatic interaction

2.1 Defining homogeneity in mixtures

In order to understand the concept of assimilation, we first have to define a few basic concepts related to mixtures. Namely, a terminological demarcation has to be made between homogeneous and heterogeneous mixtures, which can be defined either purely compositionally or relative to their phase states. In this study, we define homogeneity in mixtures in terms of their compositional characteristics. Chemical heterogeneity is also often intrinsically linked to phase heterogeneity in multi-component magmatic environments.

An even more important demarcation between homogeneous and heterogeneous mixtures is the issue of sampling scale. The size of samples or 'sample resolution' may dictate whether a system is considered homogeneous or heterogeneous as all materials composed of multiple substances can be defined as compositionally heterogeneous if the sample resolution is adequately small. For the purpose of describing homogeneity in magmatic environments we focus our treatment on spatial scales greater than typical magmatic diffusive scales that are on the order of millimeters to centimeters (see Spera et al., 2016). At such scales, the composition of a

homogeneous mixture at any location corresponds to its average composition. This definition applies to the end-member modes of magmatic interaction discussed in section 2.4.

2.2 Terminology of mixing in magmatic systems

Although mixing, hybridization, and mingling are key concepts related to the compositional evolution of magmas in almost all geotectonic environments, the terms are often used ambiguously and rather loosely in petrological literature. It is important to be precise about which sub-systems are being handled, what the controlling processes are, and what types of compositional changes are imposed on those sub-systems. In some studies of magmatic systems, complete chemical mixing of two end-members resulting in a homogeneous mixture has been called hybridization or complete hybridization (e.g., Sparks & Marshall, 1986; Spera et al., 2016). In others – like those that describe different magmatic interactions in the field – chemical mixing has simply been called mixing to distinguish it from solely physical mixing, that is, mingling (Fig. 1a and b; see section 2.4; e.g., Metcalf et al., 1995; Clemens & Stevens, 2016). To add to the confusion, some studies consider mingling as a type of hybridization (e.g., Asrat et al., 2003; Burda et al., 2011).

In the petrological literature, Oldenburg et al. (1989) first proposed quantitative metrics to describe mixing in convectively driven magma bodies. Later studies by Petrelli et al. (2006, 2011), and Spera et al. (2016) showed how various metrics could be used to study interactions of two distinct melts. Following Spera et al. (2016), we consider melt mixing to be the umbrella term that encompasses the spectrum between the following end-member processes: a) hybridization (formation of a single homogeneous melt by the chemical mixing of two end-member melts) and b) physical mixing (mingling) without chemical mixing. Therefore, mixing involves interaction of two melts in the recommended approach; the end-result can be hybridization, mingling, or something in between (see section 2.4).

2.3 Mixing vs. assimilation

Our division between magma mixing and assimilation processes is related to the degree of solidity – or melting – of the other entity taking part in the magmatic interaction process. Practical difficulties of strict definitions of mixing in magmatic systems (hybridization or mingling) and assimilation arise from the gradational character of these processes in nature. To illustrate the gradational nature, a melt (entity A in Fig. 2a) intruding a hypothetical magmatic environment with spatial variations between completely solid and completely molten material (entity B in Fig. 2a) is considered. The distribution of liquid and crystals gradually varies upwards through the system from a completely solid lowermost part to a completely liquid uppermost part. Such an environment describes, for example, magmas in which varying degrees of crystallization and crystal accumulation have taken place or partially molten migmatite complexes deep in the crust. If another genetically unrelated (ruling out a replenishment/recharge scenario of syngenetic magmas) and compositionally distinct melt (entity A in Fig. 2a) were to intrude this system, penetrating all layers, a broad array of different kinds of interaction scenarios would ensue. Within square 1 in Fig. 2a, where the intruding melt is in contact with 100% liquid material, a hybridization or mingling process is possible (see Fig. 1a–b). Within square 2 in Fig. 2a, where the melt is in contact with 100% solid material (i.e., wallrock), a "classical" case of assimilation (see Fig. 1c) or, if there were

no chemical exchange, stoping (see Fig. 1d) would take place. Everything in between these extremes describes the spectrum of interactions between liquids and solids (and, potentially, fluids) that could take place between entities A and B in Fig. 2a in nature. The overarching processes, the end-member modes of magmatic interaction (cases 1A–D in Fig. 2b), are defined and discussed in the following section.

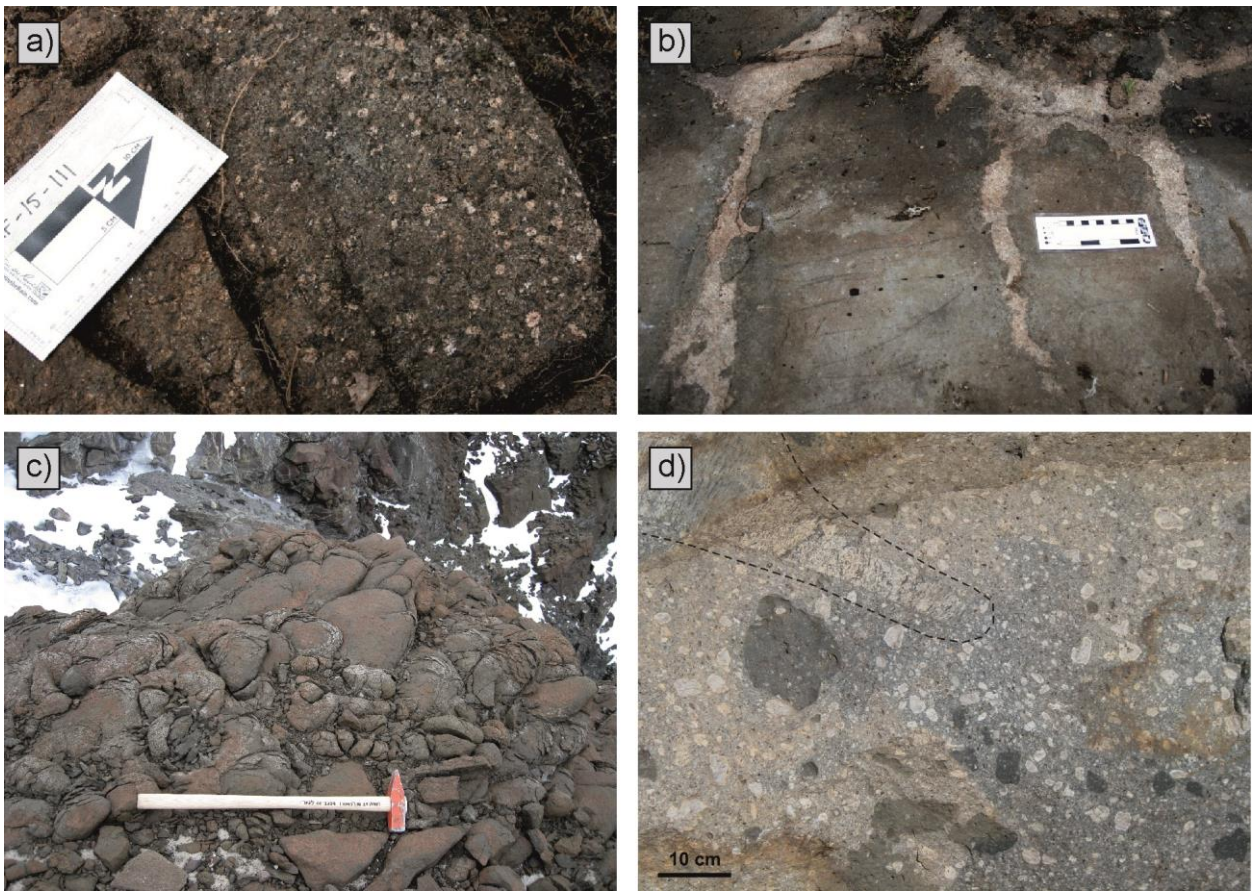

Figure 1. Textures and structures of rocks that illustrate a range of magmatic interaction processes. a) A natural example of a product (quartz monzodiorite) of magmatic interaction dominated by hybridization from the Proterozoic Ahvenisto complex in SE Finland. The composition of the dark groundmass is a mixture of monzodioritic and granitic end-member melts, and the pink alkali feldspar crystals are "inherited" from the granitic magma that was already partially crystallized at the time of interaction. The length of the arrow is 10 cm. b) A natural example of mingling of two immiscible magmas, one with monzodioritic (dark pillows) and the other with granitic (pink veins) composition, also from the Ahvenisto complex. The length of the scale bar is 10 cm. Compositional evolution of the mafic end-member magma and the style and the timing of intrusion most likely dominated the interaction process in a and b; for more details, see Fred et al. (2019). c) An outcrop of continental flood basalt flow from the Antarctic extension of the ~180 Ma Karoo large igneous province. Some of the basalt types show trace element and isotopic evidence of up to 15 wt.% of assimilation of Archean crust (Heinonen et al., 2016), but in the field, the rocks are homogeneous and do not show relict features (e.g., xenoliths or xenocrysts) of the interaction with the wallrock. The length of the hammer is ~50 cm. d) Evidence for different types of magmatic interactions in a single outcrop of a granitic rock of the 17–15 Ma Spirit Mountain batholith, southern Nevada (Walker et al., 2007). More mafic magma mingled with the more felsic magma and formed the dark pillows. A xenolith composed of gneissic country rock (surrounded with a dashed line in the upper left corner of the image) has been engulfed by the magma.

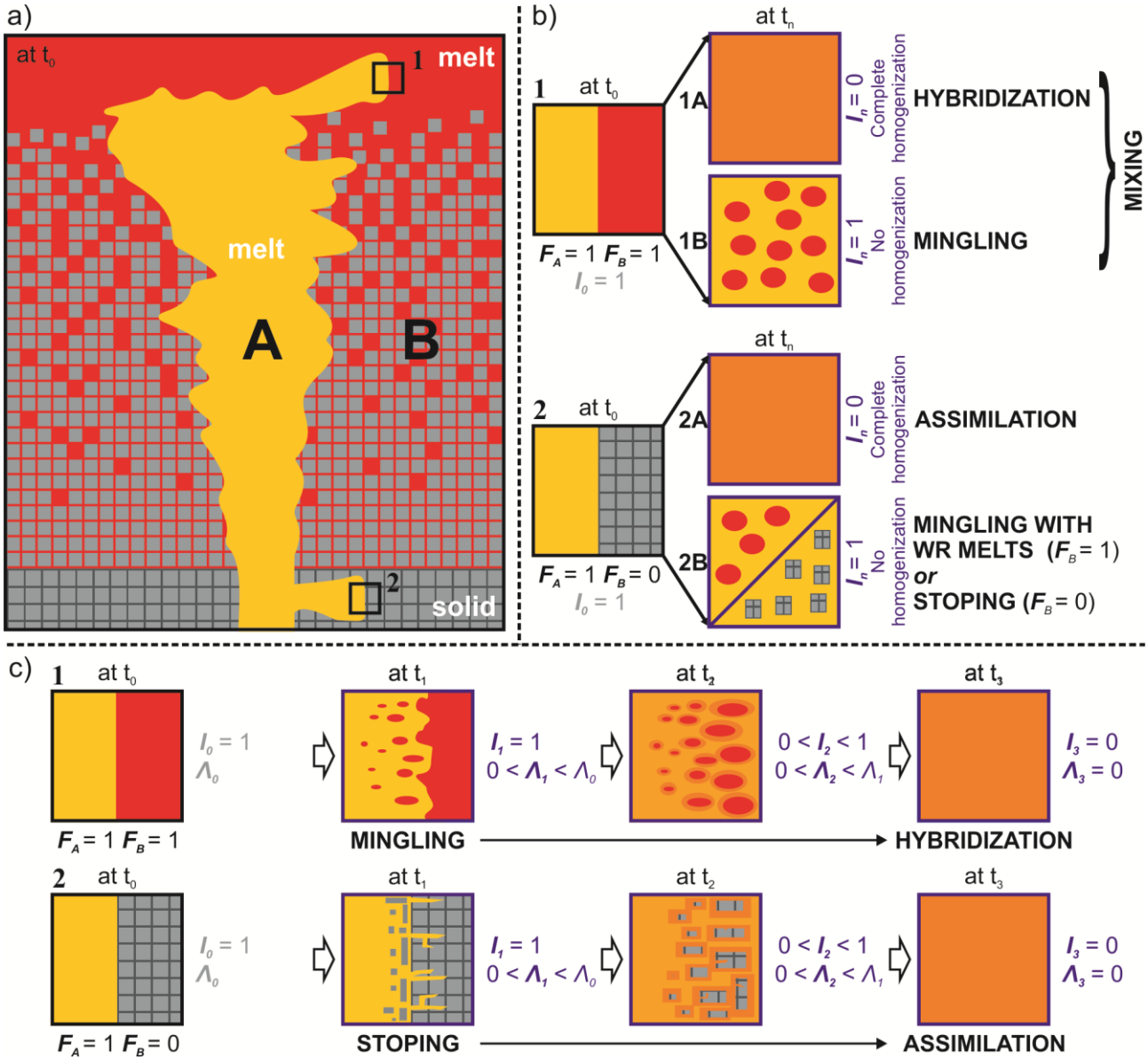

Figure 2. a) A schematic and simplified model illustrating a melt (A; in yellow) intruding a genetically unrelated environment (B) composed of solid (i.e. wallrock) at the bottom (in grey), melt at the top (in red), and a mixture of solid and melt in between. After t_0, the intruding melt is not thoroughly homogenized and thus the squares can subsequently be considered as separate systems. b) The squares demonstrate the definitions of the end-member modes of magmatic interaction according to squares 1 and 2 in a: t_0 and t_n mark the initial and later states of the system, respectively, *F* refers to melt fraction, and *I* stands for intensity of segregation of the system at the observed scale. Comparison to a reveals the gradation of mixing processes to assimilation/stoping. c) The squares demonstrate the temporal evolution and gradation from mingling to hybridization (upper set of squares) and from stoping to assimilation (lower set of squares) with the help of linear scale of segregation (Λ). Other parameters are as in b. Note that the process definitions in b and c do not allow crystallization, fluid separation, newly formed immiscible liquids, or compositionally heterogeneous wallrock (the latter in the case of stoping). For more details, see section 2.

2.4 Defining the end-member modes of magmatic interaction

2.4.1 The intrinsic parameters

In order to conceptually distinguish hybridization, mingling, and assimilation as end-member modes of magmatic interaction, we focus our investigation on the initial (t_0) and later (t_n) states of the system (Figs. 2 and 3). The "later state" should not be confused with the final or equilibrium state, as the system may evolve from physically separated (mingled) magma-magma system to a chemically mixed uniform magma, if thermal equilibration of the two magmas is attained (see Fig. 1a and b) and reactive processes (Farner et al., 2014) do not restrict mixing. Rather, the later state is a "snapshot" of the system after an arbitrary degree of interaction has occurred. Depending on the rate of cooling and other physico-chemical factors, the "final" completely crystallized products (i.e., rocks) of the different processes may preserve traces of one or several t_n states of the system (Fig. 1), but the majority of these infinite states get overprinted during polybaric ascent, cooling, and crystallization.

At t_0, the system consists of a melt body (entity A) that intrudes into surroundings composed of vertically varying amounts of liquid and solid rock material (entity B) as described in the previous section (Fig. 2). Three important measures are utilized in the following discussion: melt fraction (F), linear scale of segregation (Λ), and the intensity of segregation (I). F is simply the fraction of melt in A or B and has a value of $0 \leq F \leq 1$. The segregation parameters, which measure spatial patterns of heterogeneity, were developed for chemical reactor analysis by Danckwerts (1952, 1953) and introduced to geology by Oldenburg et al. (1989). Λ is defined as:

$$\Lambda = \int_0^{r^*} R(r)dr \qquad (1)$$

where

$$R(r) = \frac{\overline{(X_1-\bar{X})\times(X_2-\bar{X})}}{\overline{(X_i-\bar{X})^2}} \qquad (2)$$

The correlation function R is based upon the deviations of a compositional variable (X; e.g., oxide or trace element concentration) from the mean composition ($\bar{X}$); the subscript i denotes any point in the mixing domain and the subscripts 1 and 2 denote two points separated by distance r. The correlation function is then integrated over all values of r between 0 and r^*, which denotes the distance at which a perfect random correlation exists. In short, Λ quantifies the mixing state of the system in terms of the "clumpiness" of heterogeneities, is dependent on the size and shape of the heterogeneities, and is initially equal to the maximal linear scale depending on the pre-mixing configuration. If stirring of the mixture continues to infinity and the clumps break down progressively until they become vanishingly small, Λ evolves towards zero (Fig. 2c).

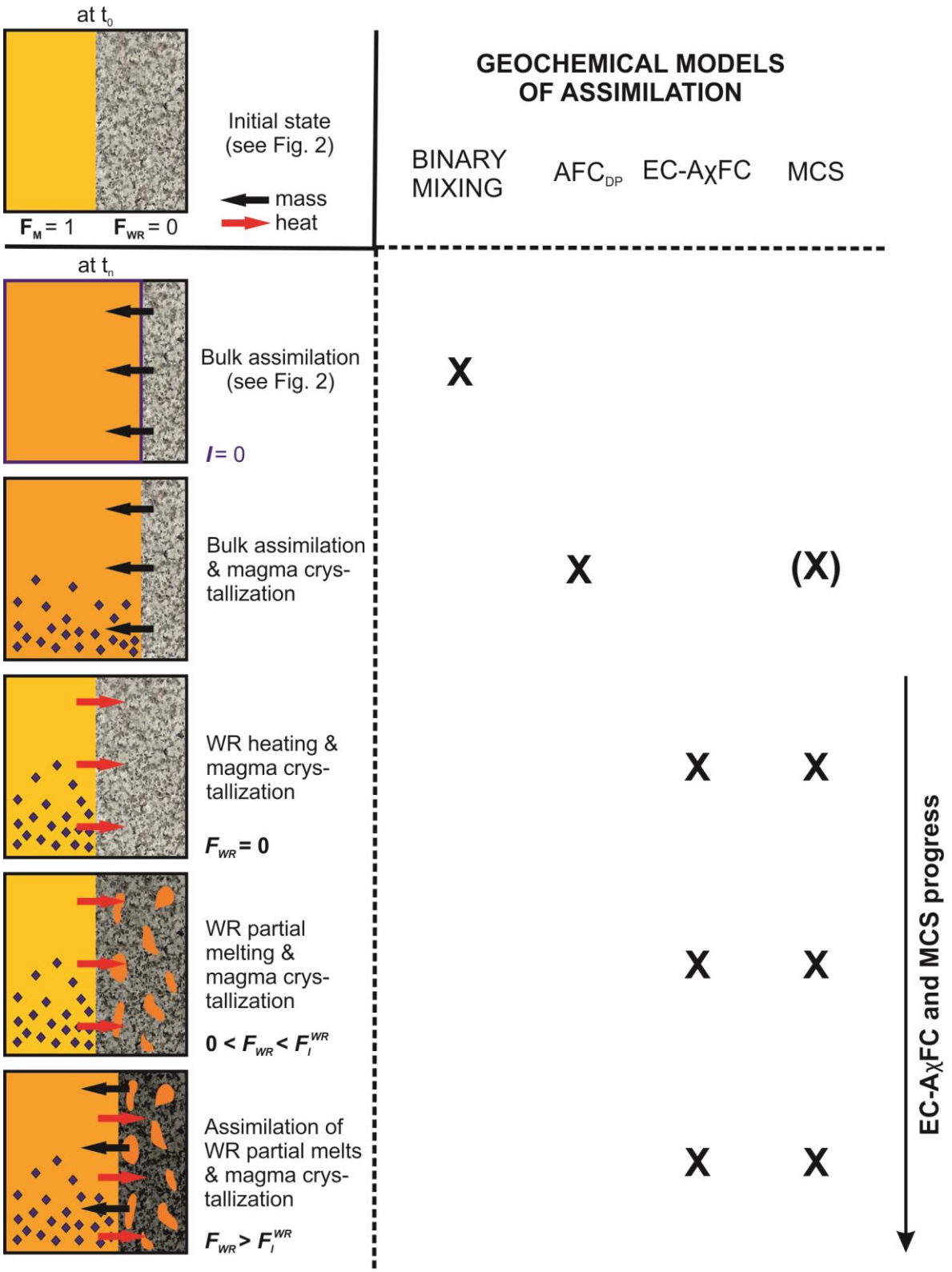

Figure 3. Schematic models illustrating processes at t_n resulting from an initial state of a melt and a solid wallrock at t_0 (see Fig. 2). The compatibility of the processes to the geochemical models of assimilation discussed in this paper are marked with an X. The X in parentheses highlights the case in which assimilation is modeled in MCS as bulk assimilation of a stoped wallrock block input as a "recharge magma" (see section 3.4). The higher the initial magma T (and the initial wallrock T) relative to wallrock solidus T, the farther the EC-AχFC and MCS models proceed. F_l^{WR} is the melt percolation threshold of the wallrock; for other variables, see section 2.4 and Fig. 2.

In contrast to Λ, I is a purely scalar measure of homogeneity and is completely independent of the shape, spatial distribution, or relative amounts of the possible heterogeneities. I is defined as:

$$I = \frac{\overline{(X_i - \bar{X})^2}}{((\bar{X} - X_A) \times (X_B - \bar{X}))} \qquad (3)$$

where X_A and X_B denote the compositions of the pure end-members A and B. I thus records the compositional variance of the system divided by the variance before mixing and can have values $0 \leq I \leq 1$ (assuming neither precipitation nor exsolution happen concurrently with mixing). In the coalescence of two compositionally distinct entities, for $I = 1$, entity A stays completely separated from entity B and the mixture is fully heterogeneous at a relevant scale. In contrast, for $I = 0$, entities A and B have formed a compositionally homogeneous mixture and no discernible heterogeneities or "clumps" of either A or B exist at the given scale. For more detailed explanations of Λ and I in relation to geological processes, the reader is referred to Oldenburg et al. (1989), Todesco and Spera (1992), and Spera et al. (2016).

2.4.2 End-member modes of magmatic interaction

To define the end-member modes of magmatic interaction, we first consider a system that is composed of two compositionally distinct homogeneous melts or a compositionally distinct homogeneous melt and a solid (squares 1 and 2 in Fig. 2a). At t_0, melt-melt interaction can be separated from melt-solid interaction on the basis of the present melt fraction (F). In the end-member modes hybridization (case 1A in Fig. 2b) and mingling (case 1B), both F_A and F_B are 1 at t_0, but for hybridization $I = 0$ and for mingling $I = 1$ at t_n. In the end-member mode of assimilation (case 2A), F_A is 1, but F_B is 0 at t_0 and $I = 0$ at t_n, denoting complete "assimilation" of a given portion of wallrock by the melt. Also, for $F_A = 1$ and $F_B = 0$ at t_0, mingling with wallrock melts ($I = 1$ and $F_B = 1$ at t_n) or stoping ($I = 1$ and $F_B = 0$ at t_n) can also be defined (case 2B). Almost any variations between the end-member modes are possible, i.e., at t_0, $0 \leq F_A < 1$ and $0 \leq F_B \leq 1$ and at t_n, $0 \leq I \leq 1$ (Fig. 2), and the resulting exchange of different elements and their isotopes between the initial end-members is governed by mass balance (in the absence of kinetic considerations). In utilizing Λ, it is possible to examine the temporal relationships of the end-member processes. At an early stage of magmatic interaction (at t_1 in Fig 2c), the melts or the melt and the solid may be fully separated, but as the time progresses, complete homogenization of the system may take place (at t_3 in Fig 2c).

There are obvious limitations in the applicability of Λ and I in describing magmatic interaction in nature: simultaneous crystallization, fluid separation, or newly formed immiscible liquids are not included in the definitions above. For example, $I = 0$ at t_n does not allow for any additional compositional heterogeneity to have emerged within the system in cases 1A and 2A at the given scale. Because I is a scalar variable, it could be defined only for the liquid(s), but this approach is also hampered by crystallization causing compositional change within the residual melt(s), potentially resulting in X_i values not within the range X_A–X_B in any of the cases at t_n (and I for the liquid thus giving values outside of the range 0–1). Given that mixing and assimilation are almost always accompanied by crystallization (see Fig. 3; for special cases of mixing causing cessation of crystallization in binary eutectic systems, see Spera et al., 2016), melt A would generally have to be superheated in the pure 1A or 2A cases to prevent crystallization. Clearly these

four cases represent highly idealized examples that could be viewed as extreme end-member approximations of natural processes. Nevertheless, they provide a framework for describing magmatic interactions that are relevant for modeling (Fig. 3) and have taken place in natural igneous systems (Fig. 1).

A potentially useful way to make the distinction for processes that are somewhere between the presented end-members would be to utilize critical melt fraction (F_c) for the entity B at t_0 (Fig. 2). Above this composition- and condition-dependent critical melt fraction (see, e.g., Arzi, 1978; van der Molen & Paterson, 1979), the crystalline framework that holds the rock together collapses, and the rock behaves more as a liquid that contains suspended crystals (i.e. $F_c \leq F_B \leq 1$: subsequent interaction with A could be called magma mixing) than a solid, which is the case when F_c is below the critical value (i.e. $0 \leq F_B \leq F_c$: subsequent interaction with A could be called assimilation or stoping). On the other hand, the initial state of the entities may be difficult to define in many natural cases. Any interaction evidenced by rocks or included in modeling can nevertheless be named as a combination of the relevant end-member modes or on the basis of the mode suspected to dominate the interaction on the basis of petrological and/or geochemical evidence (see Figs. 1 and 2). For example, although the EC-AFC and MCS models mostly consider assimilation of wallrock partial melts instead of bulk assimilation of the wallrock (Fig. 3; see sections 3.3 and 3.4), the governing mode of magmatic interaction still most closely corresponds to the end-member process 2A in Fig. 2. For determining I in such a case, X_B in equation 3 should represent the wallrock partial melt composition just before the interaction takes place. As another example of a reasonable flexibility of the naming convention, terms like "mixing with fluids" or "assimilation of fluids" can also be used, if entity B largely consists of fluid(s).

The dynamic and thermodynamic constraints for pure mixing and mingling processes as defined here are discussed in detail in Spera et al. (2016; see also Spera & Bohrson, 2018) and will not be considered further. Rather, the following discussion will concentrate on geochemical (± thermodynamical) modeling of assimilation (± crystallization). Finally, we would like to emphasize that in any of the defined processes, it is important to recognize that the final composition of the resulting mixture is governed by the mass balance of individual elements and oxides in the interacting entities. Therefore, if magmatic interactions are considered important for a particular igneous system, it should always be specified with respect to what element (or other feature) this impact is defined.

3 Overview of geochemical models of assimilation

Several studies have discussed the geochemical modeling of assimilation either in purely chemical terms (mass balance of different elements) or by including some considerations of the effects of thermodynamics or other constraints (energy balance of the system) on the process. Here we concentrate on three widely used models (binary mixing, AFC_{DP}, EC-AχFC) and the most recent and the most comprehensive model (MCS). The models are reviewed on the basis of the most influential properties in Table 1 and in Fig. 3. The outcomes of the different models for a representative assimilation case are presented and compared in section 3.5.

Table 1
A Review of Geochemical Models of Assimilation.

Model*	Components/ subsystems	Progress variable	Input constraints	Geochemical output	Improvement relative to the previous model
Binary mixing	Two compositional end-members	End-member fraction	Composition	Major and trace elements, isotopes	-
AFC_{DP}	Magma body, cumulate reservoir, and bulk wallrock	Residual melt fraction of magma	Composition, rate of assimilation relative to rate of crystallization, partition coefficients for trace elements in magma	Trace elements and radiogenic and O isotopes	Recognizes clear link between crystallization and assimilation
EC-AχFC	Magma body, cumulate reservoir, and wallrock	Resident magma temperature	Initial thermal constraints, specific heat, enthalpy of fusion/crystallization, composition, and partition coefficients for trace elements in magma and wallrock; proportion of wallrock melt entering the magma	Trace elements and radiogenic and O isotopes	Accounts for bulk thermodynamics of the system and progressive partial melting of the wallrock
MCS	Magma body, cumulate reservoir, and wallrock	Resident magma temperature	Pressure of the system (isobaric); initial thermal constraints, composition, and phase-specific trace element partition coefficients for magma and wallrock; melt percolation threshold for wallrock	Major and trace elements, phase equilibria, and radiogenic and O isotopes	Calculates thermal properties using MELTS engine; includes major elements and phase equilibria that are calculated for the magma and wallrock each temperature step; phase-specific trace element partition coefficients

*See more detailed discussion in section 3. Note that the recharge option is not included in this comparison but is available in some models.

3.1 In Bunsen's footsteps – simple binary mixing model

The concept of mixing in igneous petrology was first discussed by Bunsen (1851), who suggested that the major element compositions of certain volcanic rocks in Iceland result from hybridization of varying proportions of the most primitive and the most evolved lavas (see also Langmuir et al., 1978; Wilcox, 1999). Bunsen hypothesized that two end-member magmas, basaltic and rhyolitic, are present as separate layers below Iceland and mix during ascent (see case 1A in Fig. 2b). The same idea of binary mixing of two compositional end-members was also adopted for geochemical modeling of assimilation (e.g., Bell & Powell, 1969; Faure et al., 1974; Vollmer, 1976; see case 2A in Fig. 2b), regardless of the early realizations that substantial energy is required to heat and assimilate wallrock (e.g., Bowen, 1928; Wilcox, 1954). Binary mixing of end-members (here melt and wallrock) can be chemically quantified as:

$$X_M = f_M^0 X_M^0 + (1 - f_M^0) X_{WR} \qquad (4)$$

where X_M is the concentration of an element in the homogenized melt, X_M^0 and X_{WR} are the respective concentrations of the element in the parental melt and wallrock, and f_M^0 is the fraction of parental melt in the mixture. For the isotopic composition of the element in the mixture (ε_M), the isotopic composition of the parental melt (ε_M^0) and wallrock (ε_{WR}) are needed and the respective equation can be formulated as:

$$\varepsilon_M = f_M^0 \left(\frac{X_M^0}{X_M}\right) \varepsilon_M^0 + (1 - f_M^0) \left(\frac{X_{WR}}{X_M}\right) \varepsilon_{WR} \qquad (5)$$

In element vs. element diagrams, binary mixing models are straight lines, but in ratio vs. element or ratio vs. ratio diagrams, they are hyperbolae, unless the end-members have uniform elemental ratios (i.e., K = 1 in Fig. 4). If the element and isotopic compositions of the end-members are known, the mixing ratio of the end-members can be determined by the position of the mixture composition on the mixing line/curve (Fig. 4a). Equations 4 and 5 are compatible with the pure end-member case of assimilation (2A) in Fig. 2b (see also Fig. 3). Because assimilation is almost always accompanied by crystallization in nature (section 2.4.2), utilization of more complex equations and input is required for the modeling.

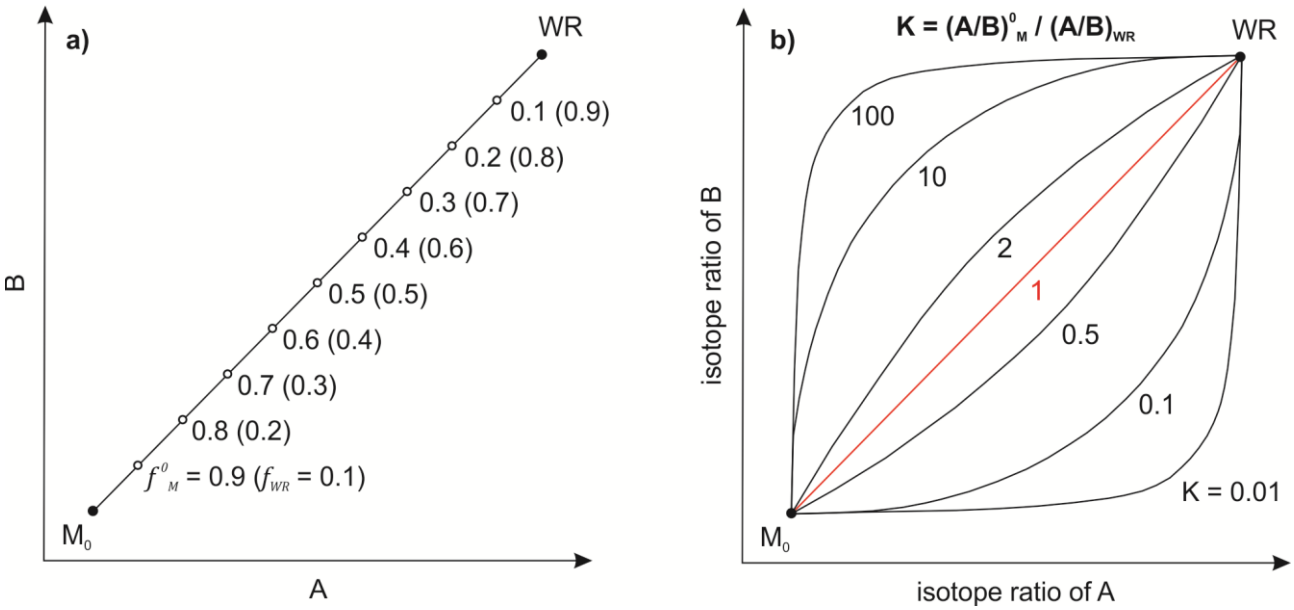

Figure 4. Magma-wallrock binary mixing models in an element A vs. element B concentration plot (a) and in a plot of their respective isotopic ratios (b). f_M^0 and f_{WR} are only given in a. In b, the different curves indicate different ratios of element A vs. element B concentrations in the magma and the wallrock (note the definition for K).

3.2 Assimilation coupled with fractional crystallization – AFC_{DP}

The simultaneous compositional effects of assimilation and fractional crystallization are taken into account in the AFC_{DP} equation (DePaolo, 1981) (Fig. 5; for earlier approaches, see O'Hara, 1977; Allégre & Minster, 1978; Taylor, 1980):

$$X_M = X_M^0 \left[F^{-z} + \left(\frac{\mathrm{r}}{\mathrm{r}-1} \right) \left(\frac{X_{WR}}{z X_M^0} \right) (1 - F^{-z}) \right] \quad (6)$$

where X_M is the concentration of a trace element in the contaminated crystallizing resident melt, X_M^0 and X_{WR} are the respective concentrations of the trace element in the parental melt and wallrock, F is the residual melt fraction relative to the parental melt, r is the rate of assimilation (mass/unit time; $\mathrm{r} \neq 1$) divided by the rate of crystallization (mass/unit time) within an F step, and $z = (\mathrm{r} + D - 1)/(\mathrm{r} - 1)$, where D is the bulk partition coefficient for the trace element in the magma. The progress variable in the $\mathrm{AFC_{DP}}$ equation is F (Fig. 5a).

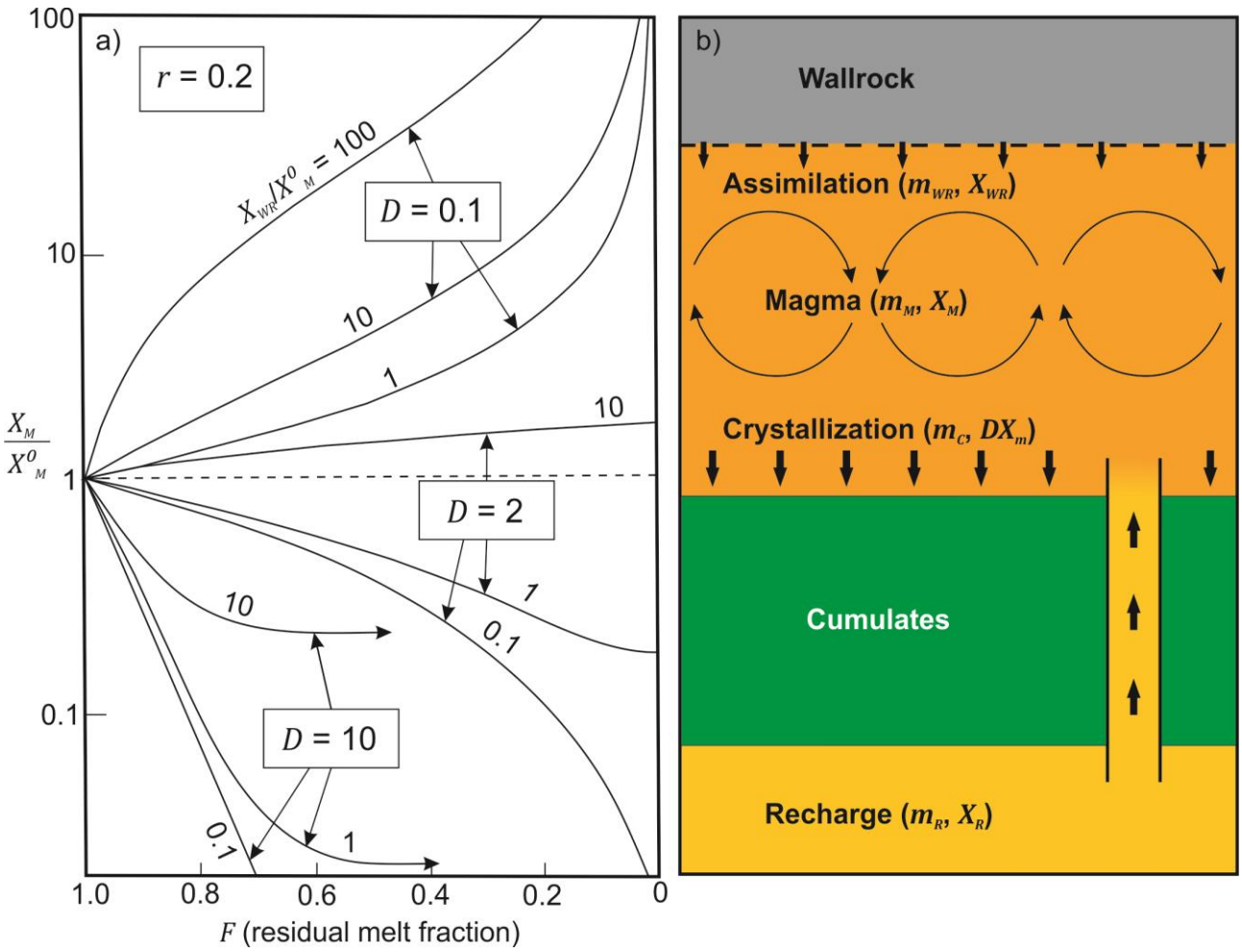

Figure 5. a) A diagram showing the evolution of X_M/X_M^0 in $\mathrm{AFC_{DP}}$ models with constant r (0.2) but with different values of bulk solid-melt partition coefficient for the magma (D = 0.1, 2, and 10) and X_{WR}/X_M^0 (0.1, 1, 10, and 100; the latter only for the model with D = 0.1). Modified after DePaolo (1981). b) A graphical illustration of the $\mathrm{RAFC_{DP}}$ model displaying the relations of the different reservoirs. The circular arrows indicate that the resident melt is constantly homogenized by convection. The thick arrows are mass flow vectors between reservoirs. Modified after DePaolo (1985).

For the isotopic composition of the trace element in the resident melt (ε_M), the isotopic composition of the parental melt (ε_M^0) and wallrock (ε_{WR}) are needed and the respective equation can be formulated as:

$$\varepsilon_M = (\varepsilon_{WR} - \varepsilon_M^0)\left[1 - \left(\frac{X_M^0}{X_M}\right)F^{-z}\right] + \varepsilon_{WR} \quad (7)$$

The AFC_{DP} equation was later extended to include simultaneous melt recharge (i.e., replenishment; $RAFC_{DP}$; DePaolo, 1985). The compositional effects of continuous addition of recharge melt into the AFC system (Fig. 5b) are incorporated into the equation based on the formulation of O'Hara (1977). If desired, periodic recharge pulses may be accomplished by running the simple AFC_{DP} model until a given F, and then treating a recharge event as a simple hybridization process between the resident melt and the recharge melt. The resulting completely hybridized melt would then be modeled using equation 6 again until the next recharge event.

It is important to point out that equations 6 and 7 are only applicable to trace elements and their isotopes (O isotopes can be modeled with some generalized assumptions; see DePaolo, 1981), and major elements need to be modeled separately. Constraining appropriate D values nevertheless requires some knowledge of the fractionating phase assemblage, which is generally based on either petrography and/or major element modeling. AFC_{DP} models generally assume a uniform D value for the modeled trace element regardless of likely changes in the fractionating phase assemblage during crystallization of the modeled system. This approach might be justified in the case of highly incompatible elements (such as Rb or Ba), but in the case of more compatible elements, especially those that are compatible in certain commonly crystallizing minerals (such as Sr in anorthitic plagioclase in silicate systems; see section 3.5), uniform D values should be used with caution, especially in models with low F.

Two of the major limitations of the AFC_{DP} equation are that the ratio of mass flow into and out of the magma body is constant across all F values and that the wallrock is treated as a bulk subsystem. The r value (the ratio of the "rates" at which wallrock is assimilated by the magma and crystals are fractionated from it) is, in fact, simply a mass ratio of assimilation relative to crystallization. Three situations can arise: (1) for $r < 1$, more mass is crystallized than assimilated, so the magma evolves towards a solid state ($1 \geq F > 0$ for equation 6); (2) for $r = 1$, the melt mass is in a steady state and equation 6 does not give a result (crystallization is exactly balanced by assimilation, i.e. $F = 1$, which corresponds to zone refining; see DePaolo, 1981); and (3) for $r > 1$, the melt grows continuously because a greater mass of wallrock (liquid) is assimilated than of crystals fractionated ($F \geq 1$ for equation 6). The latter two situations are rarely utilized, would not be thermodynamically sustainable in the long run, and are thus not considered in the following comparisons between the models.

The most obvious example of changing mass flow ratio is when the wallrock temperature is below the solidus and latent heat of crystallization is required to provide sufficient heat to trigger wallrock melting and mass flow into the magma chamber. Unlike the magma, in which progressive crystallization takes place, the effects of progressive partial melting are not taken into account in the AFC_{DP} equation, but wallrock is incorporated into the melt at a constant composition. Such an approach contrasts the excellent field documentation of partial melting processes at the contacts of intrusive rocks (e.g., Johnson et al. 2003; Hersum et al. 2007; Benkó et al., 2015) and is thermodynamically unlikely, which underline the relevance of EC-AFC modeling tools. Some studies have attempted to overcome this issue by using partially molten wallrock as the assimilant in AFC_{DP} models (e.g., Brandon, 1989; Hansen & Nielsen, 1999; Tegner et al., 1999) – such models

are likely to be more realistic, although they do not overcome the issue of assimilant having a constant composition throughout the model.

3.3 Integration of thermodynamic constraints into modeling assimilation – EC-AχFC

In order to provide more realistic estimations of the compositional effects of not only crystallization of the magma but also partial melting of the wallrock, and variations in mass flows between the reservoirs during the AFC process, the net heat budget between the reservoirs must be conserved. Applying this constraint in turn requires knowledge of the specific heat capacities of the magma and the assimilant and the crystallization and fusion enthalpies (latent heats of crystallization/melting) of relevant magma and wallrock phases. These can be determined on the basis of experimentally defined thermodynamic data or by using a thermodynamic modeling software, such as MELTS (Ghiorso & Sack, 1995; Gualda et al., 2012), which is based on such data.

Following this approach, Spera and Bohrson (2001; see also Bohrson & Spera, 2001) introduced the first EC-AFC computational model. In this model, the magma body and wallrock are treated as thermally and compositionally homogeneous subsystems separated by diathermal and semipermeable borders to enable heat and mass flow, respectively (Fig. 6). The subsystems comprise a composite system that has adiabatic and closed borders (i.e., heat or matter transfer is not permitted) to ensure heat and mass conservation in the system. Later enhanced versions of the model include magma recharge (R) (+ formation of enclaves), eruption, constraining the fraction of anatectic wallrock melt delivered to the magma body (χ), and output on solids and anatectic melt (Spera & Bohrson, 2002, 2004; Bohrson & Spera, 2007). Regardless of the possibility to include several subsystems, the resident melt that can be replenished and contaminated by wallrock in EC-AFC models is always considered to be a homogeneous mixture (see section 2.1). Because this study focuses on modeling assimilation, we concentrate on the input and the general progression of the latest energy-constrained version (EC-RAχFC; Bohrson & Spera, 2007), but without the recharge option – for more detailed descriptions of it and the different versions available, the reader is referred to the aforementioned publications.

The development of assimilation models that are closer to the natural process requires more thorough compositional and thermal input from the user. The input in EC-AχFC is divided into physical (equilibration) and compositional (path-dependent) parameters. The thermal input consists of liquidus temperatures, initial temperatures, and specific heats of the magma and the wallrock, solidus of the composite system, and the bulk heat of crystallization for the magma and the bulk heat of fusion for the wallrock. The user can also alter melting/crystallization productivity functions and the magma temperature decrement, although default values are provided, and χ is predefined. The first stage of input is followed by a thermal simulation, after which the user can select an appropriate equilibration temperature at which equilibrium between the resident magma and wallrock is attained. Lowering the equilibration temperature corresponds to a larger mass of the input wallrock being involved in the simulation. For a standard case, the compositional input consists of concentrations of up to six trace elements, up to three isotopic compositions, and partition coefficients for these elements in the magma and in the wallrock. The partition coefficients can be temperature-dependent. In addition, oxygen isotopes are modeled by constraining O contents

and isotopic compositions of the magma and the wallrock, but assuming no isotope partitioning during melting or crystallization.

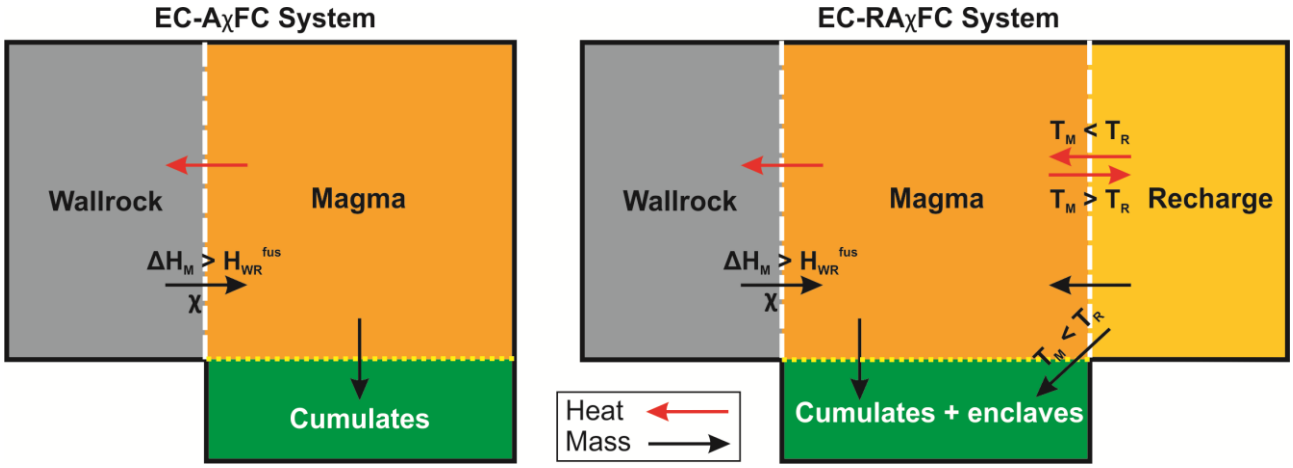

Figure 6. A schematic illustration of the thermodynamic systems (resident melt, cumulates ± enclaves, wallrock, and recharge) in the latest formulations of EC-AχFC and EC-RAχFC systems (Bohrson and Spera, 2007). The thick black line surrounding the entire composite system is an adiabatic and closed boundary, which restricts heat or mass flow. The yellow dotted lines represent adiabatic and semipermeable boundaries, through which only mass flow is permitted, and the white dashed lines represent diathermal and semipermeable boundaries, which allow both heat and mass flow. The arrows show possible directions for the heat and mass flows and special conditions for certain arrows are indicated. The abbreviations are as follows: ΔH_M = sensible + latent heat released by magma, H_{WR}^{fus} = wallrock heat of fusion, T_M = magma temperature, and T_R = recharge magma temperature, χ: fraction of anatectic wallrock melt delivered to the magma body.

In the EC-AFC system, the progress variable is the resident magma temperature that evolves towards the user-defined equilibration temperature. The thermal equilibrium is driven by the enthalpy (sensible and latent heat) of the composite system. The bulk latent heat of crystallization is approximated as a weighted average of the bulk enthalpy of crystallization at each step. The crystallized mass is transferred into the cumulate subsystem that has an adiabatic and semipermeable boundary (Fig. 6). The heat flows and distributes equally to the entire mass of the wallrock raising its temperature until its solidus is reached. After that, the latent heat of fusion of the wallrock must be surpassed in order to trigger wallrock partial melting, which is modeled as fractional melting. The fraction of the wallrock melt defined by χ is extracted from the wallrock and homogenized into the resident melt. Each wallrock melt batch added to the magma reservoir compositionally and thermally equilibrates with the resident melt instantaneously and the composition of the residual wallrock is modified accordingly. The model proceeds accordingly in user-defined temperature steps until thermal equilibrium between the magma and wallrock is reached and the run concludes.

The output of a EC-AχFC model run using the latest version (Bohrson & Spera, 2007) lists the thermal evolution of the resident magma and the wallrock; relative masses of the resident melt, cumulates, and generated and assimilated anatectic wallrock melt; melt productivity of the magma; and the trace element (± isotopic) composition of the resident melt. Additional output lists the trace element compositions of the anatectic wallrock melt and the magma cumulates. Isotope values for

cumulates or the anatectic melt identical to those of the resident melt at each step and the wallrock, respectively.

Even though EC-AFC models include heat budget and partial melting of the wallrock in the trace element and isotope calculations, the phase changes governing the available latent heat are simplified and a detailed picture of phase equilibria and energy conservation is not provided. In nature, the crystallizing and melting phase assemblages change, which lead to variations in heat production due to cooling and crystallization and, consequently, in the available energy for heating and partial melting of wallrock. Most significantly, phase changes may have profound effects on partition coefficients and hence the trace element and isotope mass exchange between the subsystems. The addition of rigorous phase equilibria calculations instead of the approximate form utilized in the EC-AFC model provides a more accurate characterization of open system magmatic evolution. This limitation of EC-AFC lead to development of the MCS model.

3.4 Phase equilibria of assimilation – MCS

Development of computational tools based on the thermodynamic properties of geologic materials to model phase equilibria in fully or partially melted silicate systems (e.g., Carmichael et al., 1977; Ghiorso, 1985; Ariskin et al., 1993; Ghiorso & Sack, 1995; Gualda et al., 2012) has been one of the most significant advances in igneous petrology of recent decades. Although the MELTS software includes a rudimentary bulk assimilation function (Ghiorso & Sack, 1995; Ghiorso & Kelemen, 1987; see also Reiners et al., 1995), the treatment of the wallrock using a composite open system approach similar to that for the parental magma had been lacking before the introduction of MCS (Bohrson et al., 2014, 2020; Heinonen et al., 2020).

Using a selected MELTS engine (currently pMELTS or rhyolite-MELTS versions 1.0.x, 1.1.x, or 1.2.x; Ghiorso & Sack, 1995; Ghiorso et al., 2002; Gualda et al., 2012; Ghiorso & Gualda, 2015), MCS models the phase equilibria and major element evolution of a composite system composed of subsystems that are crystallizing magma body, wallrock, and up to five recharge magmas. MCS utilizes the same thermodynamic system definitions as EC-RAχFC (Fig. 6) with the exception of excluding enclave formation associated with recharge events. The incremental portions of wallrock partial melt exceeding the set percolation threshold (i.e., the critical melt fraction for melt extraction to be possible) and recharge magmas are always completely equilibrated with the resident melt. If using the MELTS engines 1.1.x or 1.2.x, MCS also models the evolution of a possible fluid phase (consisting of H_2O and/or CO_2) in the subsystems. MCS is continuously being developed and reader should refer to http://mcs.geol.ucsb.edu/, where updates are announced and the latest public version is available for users.

As in the case of EC-AFC, we focus on modeling of assimilation without recharge in MCS in the following discussion. Input for MCS is a single Microsoft Excel worksheet that the software reads before commencing a run. The input consists of system variables (e.g., wallrock percolation threshold, excluded MELTS phases, pressure, and oxygen fugacity) and initial thermal and compositional parameters for the parental magma, wallrock (if included), and recharge magma (if any). The models are always isobaric and the mass of the initial resident magma is 100 non-dimensional units. Note that, due to lack of thermodynamic data, modeling of systems including carbonatitic magmas or carbonate wallrock may halt the engine. In addition, the MELTS engine

may not find feasible solutions for highly hydrous systems that show evidence of significant fractionation of, e.g., biotite or hornblende.

Like in EC-AFC models, the resident magma temperature is the progress variable in MCS; the user defines a temperature decrement that tracks cooling and crystallization of the magma body. During an MCS-AFC run, the initial temperature of the resident magma begins to decrease in user-defined steps. During each step both the amount of heat (sensible + latent heats) that homogeneously distributes into the wallrock and the equilibrium phase assemblages for the resident magma (i.e., major element compositions of stable melt + solids ± fluid phases) are calculated. The fractional crystallization of the resident magma is modeled in these steps within which crystallization takes place in equilibrium with the melt like in stand-alone MELTS platform; larger temperature steps more closely approximate equilibrium crystallization. For each temperature decrement, the equilibrium solids fractionate into a cumulate solid reservoir that remains chemically but not thermally isolated from the melt in the magma subsystem. Separation of a possible fluid phase is treated similarly to crystallization. The model proceeds as magma cools via the user-defined temperature decrement. If enough heat is transferred, the wallrock partial melting begins after which the equilibrium phase assemblages and their major element compositions are also defined for the wallrock. Unlike in the EC-AχFC model, the wallrock melt forms via equilibrium melting rather than fractional melting.

After assimilation begins, the amount of wallrock partial melt that is transferred into the magma chamber is the portion that exceeds the wallrock percolation threshold value. This wallrock partial melt batch is thermally equilibrated and chemically homogenized with the resident melt, and the next magma temperature decrement and crystallization step is performed on the resulting homogenized melt composition. The continuous extraction of wallrock partial melt results in the change of residual bulk composition and hence phase equilibria in the remaining wallrock, which becomes more mafic and refractory. The MCS model continues until the resident magma and the wallrock reach thermal equilibrium or a pre-constrained resident magma temperature or residual melt mass is achieved. MCS can also model bulk AFC by introducing a stoped wallrock block that may be composed of variable proportions of solid phases, melt, and fluid. Computationally, this process utilizes the recharge function of MCS because assimilation of a stoped block can be treated with the same thermodynamic and mathematical approach. The bulk stoped block is completely melted and homogenized with the resident melt, and the resulting contaminated magma reflects the thermodynamic consequences.

The MCS output includes the phase equilibria, major element compositions of the subsystem melts and all stable solid and fluid phases at each step, and various thermal and mass parameters of the system and subsystems. Calculations of the evolution of up to 48 trace elements and eight isotope ratios ($^{87}Sr/^{86}Sr$, $^{143}Nd/^{144}Nd$, $^{176}Hf/^{177}Hf$, $^{206}Pb/^{204}Pb$, $^{207}Pb/^{204}Pb$, $^{208}Pb/^{204}Pb$, $^{187}Os/^{188}Os$, and $\delta^{18}O$) in the resident melt, solids, and fluids can be performed. These calculations are based on equations AIV-2–4 of Spera et al. (2007) and utilize phase-specific user-input partition coefficients.

3.5 Comparison of the different assimilation models

The differences of the aforementioned models are illustrated for a representative case of a basaltic melt derived from a depleted mantle source assimilating average continental crust (compositions in Table 2). The other model parameters are listed in Table 3, except for the

extensive set of partition coefficients used for the MCS models that are listed separately in Table 4. The model results are illustrated in Figs. 7–9. Note that the AFC_{DP} and EC-AχFC models only include trace elements. EC-AχFC thermal parameters represent the standard upper crustal case of Bohrson and Spera (2001), which have been widely used in the literature (e.g., Jourdan et al., 2007; Cucciniello et al., 2010, Jennings et al., 2017; Günther et al., 2018). In the MCS model, the amount of wallrock involved is half the amount of parental magma. The input and output of the MCS model presented here can be downloaded from the MCS website at http://mcs.geol.ucsb.edu/.

Table 2
Composition End-members Used in the Assimilation Models.

	Parental Melt*	**Wallrock†**
Majors		
SiO_2 (wt.%)	50.37	66.28
TiO_2	1.77	0.63
Al_2O_3	14.07	15.26
Fe_2O_3	1.79	0.84
FeO	8.98	4.24
MnO	0.18	0.10
MgO	7.97	2.45
CaO	12.33	3.55
Na_2O	2.16	3.23
K_2O	0.23	2.77
P_2O_5	0.15	0.15
H_2O	-	0.50
Traces		
Ni (ppm)	154	47
Rb	2.4	84
Sr	226	320
Nd	10.53	27
Isotopes		
$^{87}Sr/^{86}Sr$	0.702819	0.716
$^{143}Nd/^{144}Nd$	0.513074	0.51178

* Volatile-free parental melt composition after a depleted continental flood basalt dike sample P27-AVL (Luttinen & Furnes, 2000), except for the isotopic composition that represents the mean modern MORB (Gale et al., 2013). FeO vs. Fe_2O_3 calculated from FeO^{tot} at QFM at 2 kbar with rhyolite-MELTS 1.2.0 (Gualda et al., 2012; Ghiorso & Gualda, 2015).

† Wallrock composition after average upper continental crust of Rudnick and Gao (2003), except for the addition of 0.5 wt.% of water and the isotopic composition that is the estimation of the average composition of modern river waters globally (Goldstein & Jacobsen, 1988). FeO vs. Fe_2O_3 calculated in the same way as for the parental melt.

Table 3

Physical and Thermal Parameters for the AFC_{DP}, EC-AχFC, and MCS Models and the Bulk Partition Coefficients for the AFC_{DP} and EC-AFC Models.

AFC_{DP}*		**EC-AχFC†**		**MCS#**	
r	0.5	Magma liquidus T (°C)	1280	Rhyolite-MELTS engine	1.2.0
Magma solid-melt D's		Magma initial T (°C)	1280	F_l^{WR} (FmZero)	0.1
$D(Ni)^M$	5	Wallrock liquidus T (°C)	1000	Pressure (bars)	2000
$D(Rb)^M$	0.05	Wallrock initial T (°C)	300	Magma initial T (°C)	1225
$D(Sr)^M$	1	Solidus T (°C)	900	Magma T decrement (°C)	5
$D(Nd)^M$	0.2	Specific heat of magma (J/kg·K)	1484	Wallrock find solidus: end T (°C)	680
		Specific heat of wallrock (J/kg·K)	1370	Wallrock find solidus: T decr. (°C)	5
		H of crystallization of magma (J/kg)	396000	Wallrock find solidus: start T (°C)	950
		H of melting of wallrock (J/kg)	270000	Wallrock mass (Magma = 100)	50
		χ	0.9	Wallrock initial T (°C)	300
		Equilibration T (°C)	980		
		Magma solid-melt D's		Phase-specific K_D's given in Table 4	
		$D(Ni)^M$	5		
		$D(Rb)^M$	0.05		
		$D(Sr)^M$	1		
		$D(Nd)^M$	0.2		
		Wallrock solid-melt D's			
		$D(Ni)^{WR}$	2		
		$D(Rb)^{WR}$	0.03		
		$D(Sr)^{WR}$	6		
		$D(Nd)^{WR}$	0.3		

* D values represent average values of the MCS model (Table 4)

† Thermal parameters represent the standard upper crustal case of Bohrson and Spera (2001), D values represent average values of the MCS model (Table 4), and the model has been run using non-linear logistical melting functions.

Thermal parameters defined at 2 kbar with rhyolite-MELTS 1.2.0. (Gualda et al., 2012; Ghiorso & Gualda, 2015). Note that F_l^{WR} corresponds to $1-\chi$ in EC-AχFC.

Table 4

Phase-specific Partition Coefficients for the MCS Models

	Magma solid-melt K_D's[#]				**Wallrock solid-melt K_D's[#]**			
	$K_D(Ni)^M$	$K_D(Rb)^M$	$K_D(Sr)^M$	$K_D(Nd)^M$	$K_D(Ni)^{WR}$	$K_D(Rb)^{WR}$	$K_D(Sr)^{WR}$	$K_D(Nd)^{WR}$
alkali feldspar†	-	-	-	-	0.5	0.4	5	0.02
biotite	-	-	-	-	15	3	0.5	1
clinopyroxene*	3	0.01	0.1	0.2	-	-	-	-
orthopyroxene	-	-	-	-	10	0.01	0.01	1
plagioclase†	0.1	0.1	3	0.1	0.5	0.02	10	0.2
quartz	-	-	-	-	0	0	0	0
rhm-oxide	30	0.1	0.1	0.1	5	0.04	0.1	1
spinel	30	0.1	0.1	0.1	5	0.04	0.1	1

[#] Compiled on the basis of the EarthRef database (https://earthref.org/KDD/)

* MELTS identifies two distinct clinopyroxene phases in the magma in the model, but they are treated equally in the trace element model

† Plagioclase and alkali feldspar are respectively denoted "feldspar {1}" and "feldspar {2}" in the model output

As mentioned previously, the binary mixing model results in straight lines in x-y diagrams between the end-members (Figs. 4a and 7a–c), except if distinct elemental and isotopic ratios are involved (Figs. 4b and 7d). In comparison, the inclusion of fractional crystallization in the AFC_{DP} model is illustrated by the trend not pointing towards the wallrock composition. Simultaneously with assimilation of the wallrock bulk composition, crystallization depletes the melt of compatible elements and enriches it in incompatible elements. Changes in the Sr isotope composition relative to changes in the Nd isotope composition are more dramatic for the AFC_{DP} model compared to the binary mixing model because Sr is more compatible than Nd in the solids in the crystallizing resident magma (Fig. 7d); when Sr is efficiently depleted from the resident melt, wallrock control on its isotopic composition increases. Nevertheless, both bulk mixing and AFC_{DP} models commonly use bulk country rock composition as the contaminant, which has significant but often overlooked compositional effects: incompatible trace elements get rather subtly enriched in the resident melt relative to the degree of assimilation (Fig. 7c). This is exemplified in studies on mafic systems, for which thermodynamically unfeasible amounts (several tens of wt.% relative to mass of the parental magma) of assimilation are implied by such models to explain the most contaminated trace element and radiogenic isotope compositions (e.g., Carlson, 1981; Goodrich & Patchett, 1991; Molzahn et al., 1996; Larsen & Pedersen, 2009).

In comparison to AFC_{DP}, EC-AχFC includes thermal parameters and partition coefficients for the partial melting of the wallrock. In the standard upper crustal case of Bohrson and Spera (2001), the wallrock is heated from its initial temperature (300 °C) all the way to its solidus (900 °C), which requires a significant release of latent heat via crystallization of the magma. Because of this, the start of assimilation is delayed until after about 70 wt.% of crystallization (Fig. 8b). After assimilation begins, the earliest wallrock partial melts, which are modeled by fractional melting in EC-AχFC, are loaded with incompatible elements, which results in considerable enrichment in their concentrations in the resident melt (e.g., Rb in Fig. 7c). The extracted partial melts progressively deplete the residual wallrock of incompatible elements as assimilation proceeds. For this reason, resident melt with higher degrees of assimilation may actually show relatively lower concentrations

of such elements than earlier less contaminated resident melt. This is the case for Rb here: enrichment in the resident melt caused by fractional crystallization cannot compete with dilution caused by progressive assimilation of now Rb-depleted wallrock partial melts (Fig. 7c). In contrast, an element that is compatible in wallrock (e.g., Sr in Fig. 7b) shows exactly the opposite behavior. The compatibility of Sr in the wallrock also delays the effect of assimilation on the Sr isotopic composition of the resident melt (Fig. 7d).

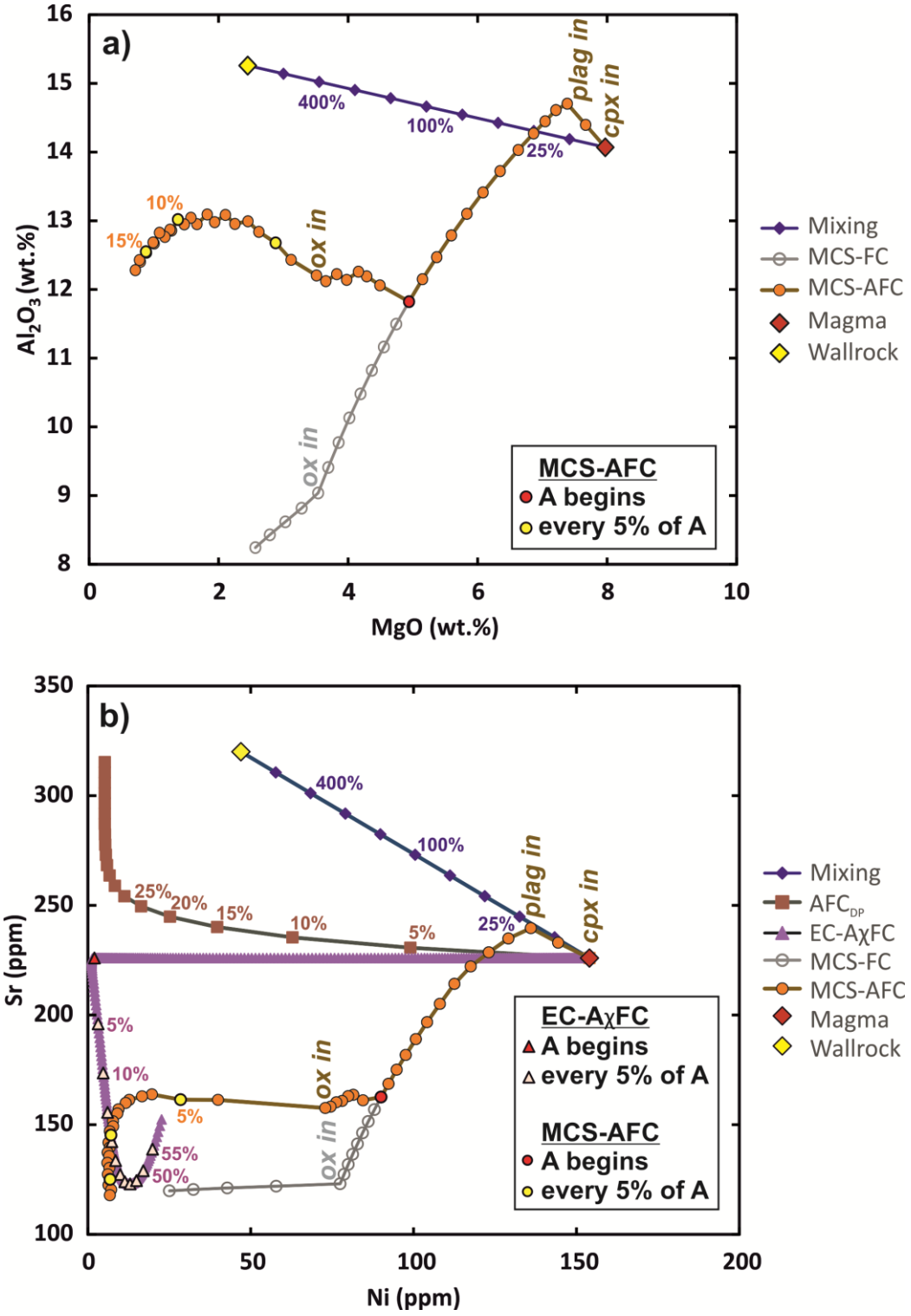

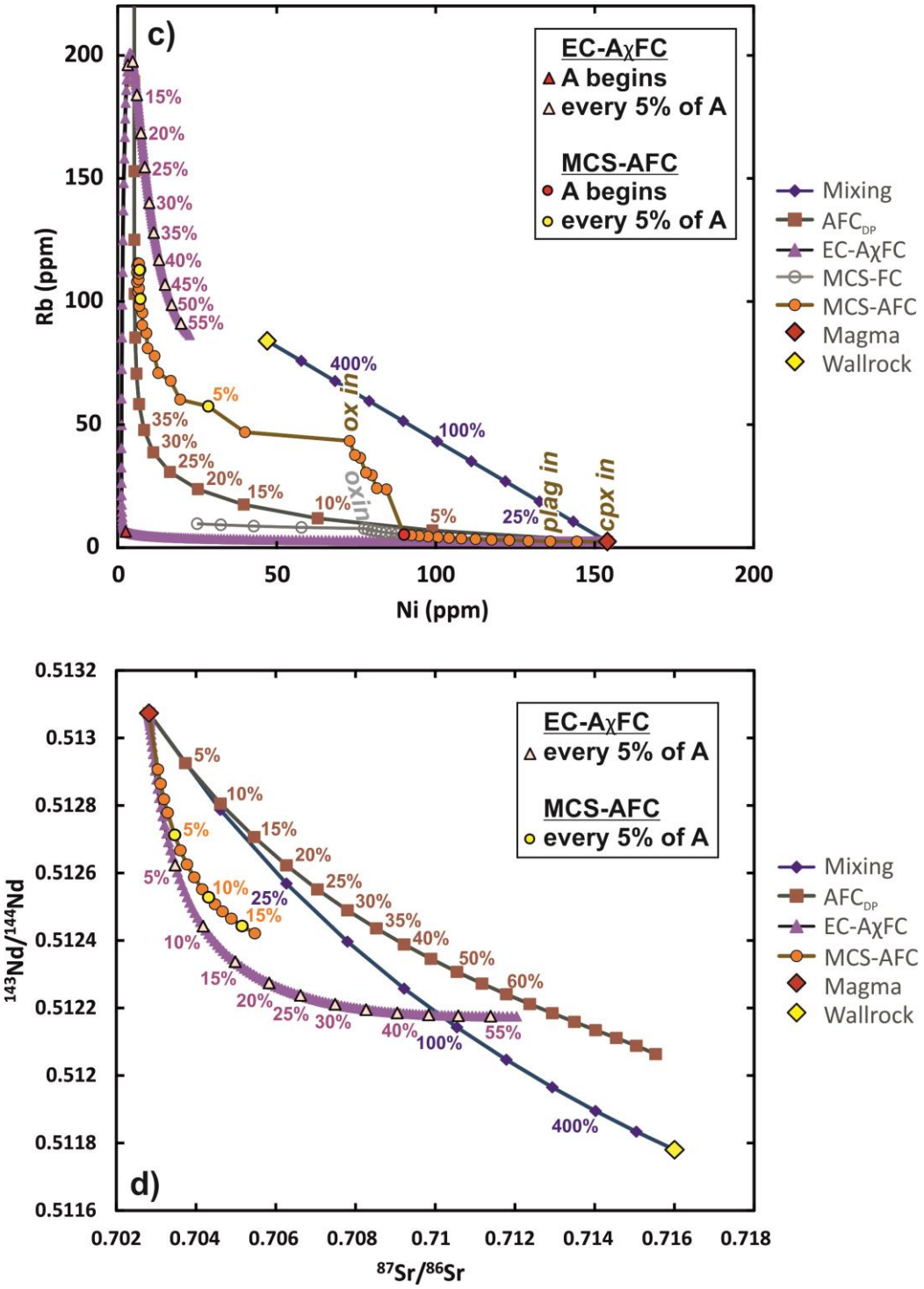

Figure 7. Outcomes of the resident melt composition of the binary mixing, AFC_{DP}, EC-AχFC, and MCS models (Tables 2–4) shown in MgO vs. Al_2O_3 (a), Ni vs. Sr (b), Ni vs. Rb (c), and $^{87}Sr/^{86}Sr$ vs. $^{143}Nd/^{144}Nd$ (d) diagrams. The presented AFC_{DP} and EC-AχFC models do not include major elements and are thus not shown in a. An MCS fractional crystallization model for the parental melt (Table 1) is shown for reference in a–c; the amount of fractionation (~80 % relative to the mass of the parental melt) in it is similar to that of the primary MCS model with assimilation. The tick marks represent additions or decrements of model-specific progress variables as listed in Table 1 and all starting from the parental melt composition: For the binary mixing model, tick marks denote an increase of 0.1 in the fraction of WR in the mixture; for the AFC_{DP} model, they denote decrements of 0.05 in *F* and increments of 0.05 in the mass of added assimilant relative to the parental melt; in the case of the EC-AχFC model, they denote ~1°C temperature decrements; for the

MCS model they denote the imposed 5 °C magma temperature decrements and the assimilation steps. Note that the mass of assimilated wallrock relative to the mass of parental melt is indicated as percentages for all models. Steps during which a new phase joins the crystallization assemblage in the resident magma are indicated for the MCS models (cpx = clinopyroxene, plag = plagioclase feldspar, ox = spinel and/or rhombohedral oxide, the latter shown for the FC and AFC_{DP} models separately), except in d.

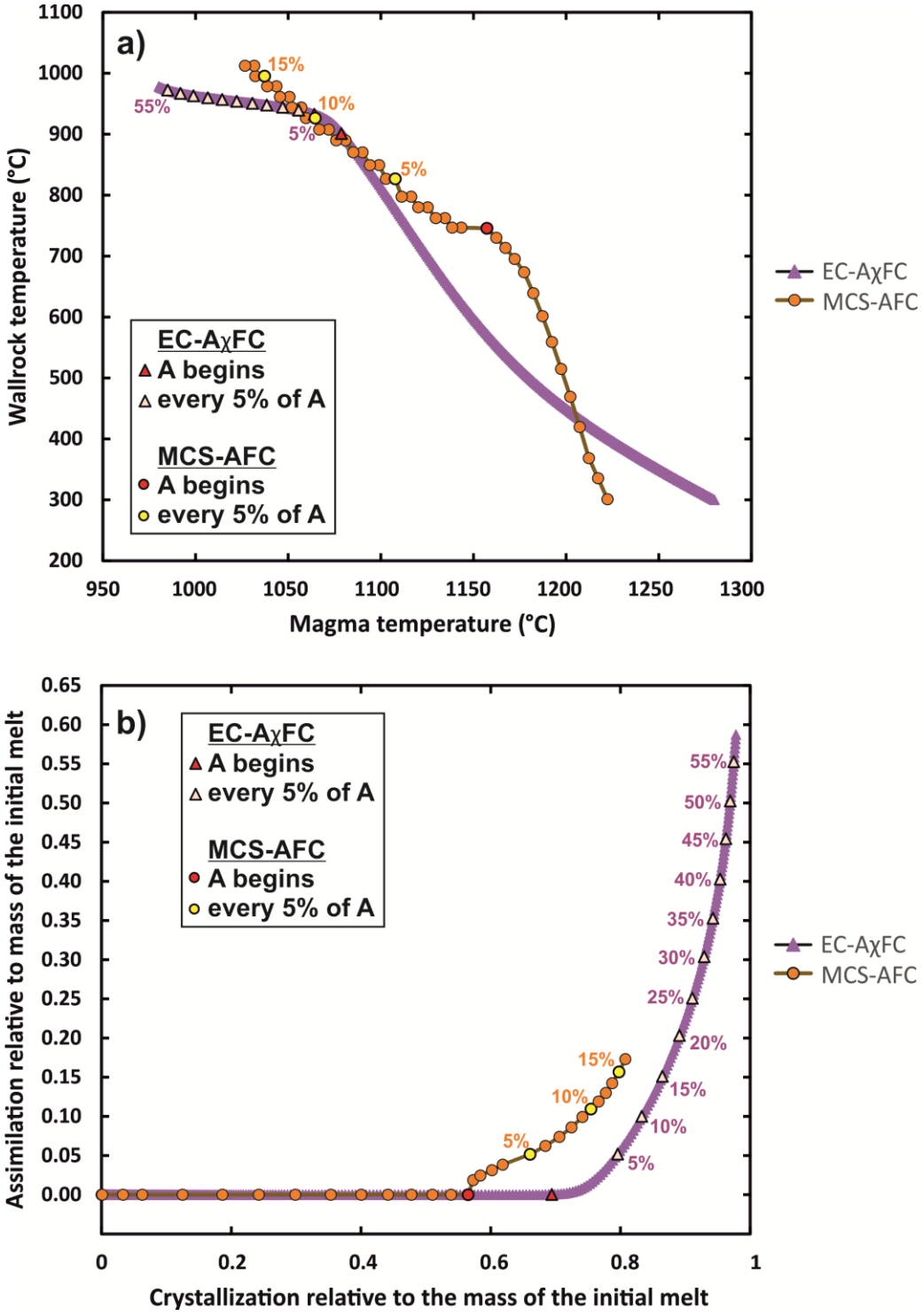

Figure 8. Thermodynamic comparisons of the EC-AχFC and MCS models (Tables 2–4) shown in magma temperature vs. wallrock temperature (a) and mass of cumulate vs. mass of assimilated wallrock (b) diagrams. See Fig. 7 for additional details.

MCS considers the evolution of phase equilibria and major elements, trace elements, and isotopes throughout the crystallization and assimilation process (Fig. 7). In addition, and like in EC-AχFC, it is not only possible to follow the evolution of the resident magma, but also the composition of the cumulate and the composition of the wallrock partial melt (which forms by equilibrium melting unlike in EC-AχFC) and the residual wallrock (Fig. 9). The output thus provides several geochemical tracers for understanding assimilation processes in various extrusive and intrusive systems. In the case of elements that show varying compatibility in stable phases (e.g., Sr and Ni; see Table 4), the assimilation trends may be considerably complex (Fig. 7b). Figure 8 illustrates how the MCS model, which takes the changing thermodynamic properties of the resident magma and wallrock within each temperature step into account, thermally differs from the standard EC-AFC upper crustal case of Bohrson and Spera (2001). The wallrock is efficiently heated by the high amount of early crystallization in the MCS model, and the solidus of the wallrock is lower and attained earlier. Comparison with a MCS fractional crystallization model (Fig. 7a–c) illustrates that assimilation may have notable effects, not only on incompatible element concentrations (Fig. 7c), but also on the major element composition of the resident melt (Fig. 7a).

The presented EC-AχFC and MCS models illustrate that considerable amounts of crystallization and heat exchange between the magma and wallrock are required before assimilation begins (Fig. 9). Movement of such magmas would obviously stall after the onset of assimilation due to their high crystal contents, unless the crystals were efficiently separated from the melt as MCS assumes. In cases where significant assimilation has obviously taken place in relatively primitive magmas, preheating of the wallrock by hydrothermal systems, previous magma pulses, or more primitive parental magma may have to be taken into consideration. Accordingly, the initial wallrock temperature may need to be set to a higher value than would otherwise be suggested, for example, based on continental geotherms (see Heinonen et al., 2016, 2019; Moore et al., 2018). Alternatively, inclusion of a lower mass of wallrock in the model could more closely replicate the initial stages of magma emplacement, where only a thin zone of wallrock is subjected to heat exchange. The mass of wallrock to be included in MCS models in different environments is extensively discussed in Bohrson et al. (2014).

It should be noted, that whereas a standard case of wallrock assimilation in MCS always requires partial melting, energy requirements for reactive bulk assimilation of disintegrated wallrock blocks may be much lower (Beard et al., 2005). This may be the case in some felsic systems, where there is less heat available for complete melting reactions to take place in the wallrock. Such cases can be modeled with stoped blocks in MCS (see section 3.4) and the result would chemically approach the result of binary mixing. On the other hand, the strong crustal chemical overprint in many basalts lacking any macroscopic evidence of assimilation (Fig. 1c; e.g., Carlson, 1991; Lightfoot et al., 1993; Larsen & Pedersen, 2009; Heinonen et al., 2016) testifies that (partial) melting of the wallrock and homogenization of these melts with the resident magma or complete digestion of stoped blocks must be a significant processes in their differentiation.

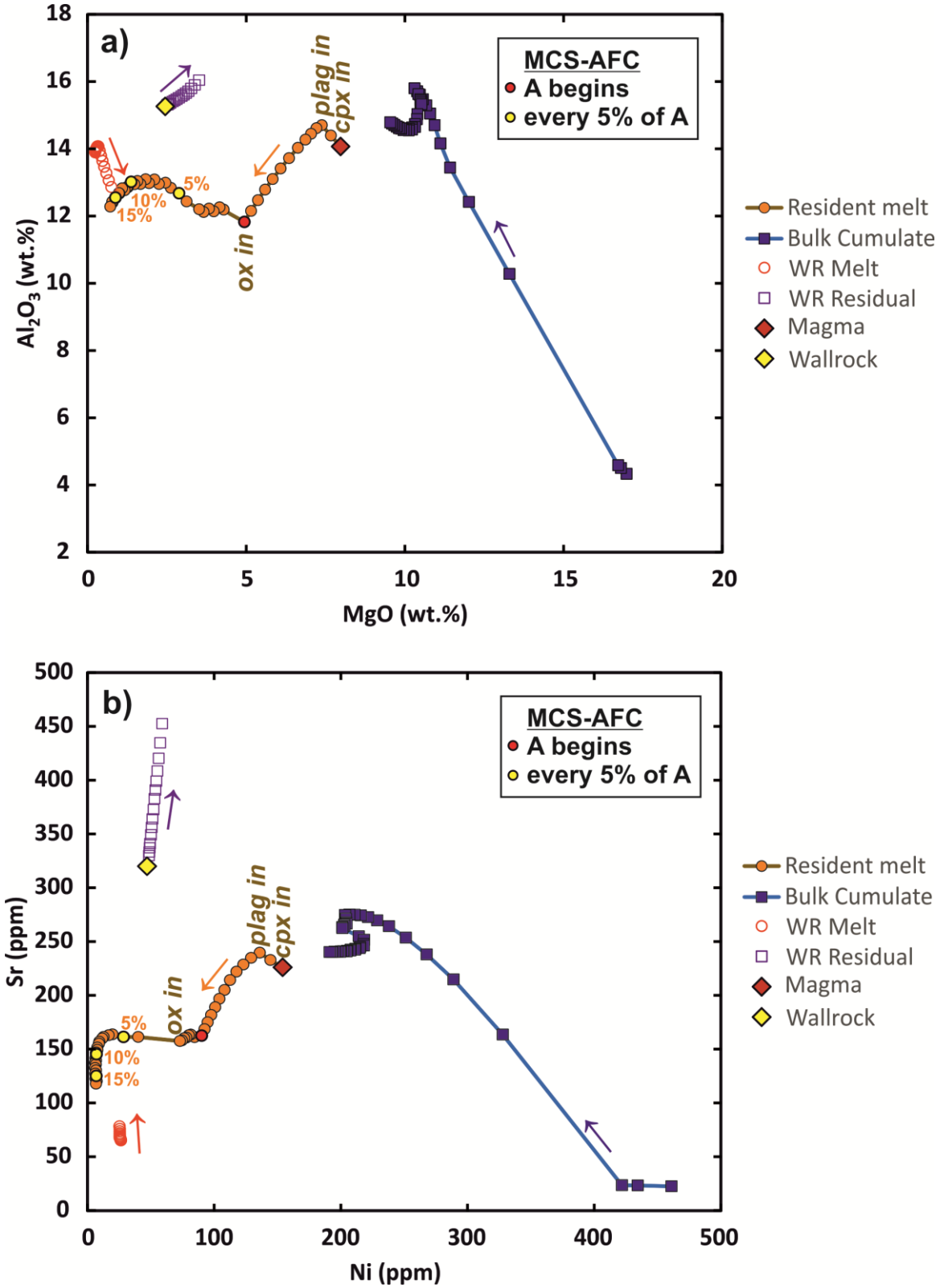

Figure 9. Outcomes of the resident melt, bulk cumulate, wallrock melt, and wallrock residual (solid + melt) compositions of the MCS-AFC model (Tables 2–4) shown in MgO vs. Al_2O_3 (a) and Ni vs. Sr (b) diagrams. See Fig. 7 for additional details.

3.6 MCS applied to a natural system: flood basalts from Antarctica

Comparisons of hypothetical models presented in the previous section illustrate the differences between the discussed methods and highlight the capabilities of MCS, but it is also instructive to provide an example of MCS applied to a natural system. Fully documenting an MCS model for a natural system requires extensive background and discussion (e.g., on the feasibility of the selected input values). Thus, for illustrative purposes we provide a short overview of already published results and modeling for Antarctic flood basalts that belong to the ~180 Ma Karoo large igneous province (see also Fig. 10). The reader is referred to the original publication (Heinonen et al., 2019) for more detailed information and for the original MCS input and output.

The lavas in question (low-ε_{Nd} CT1 magma type; Luttinen & Furnes, 2000) exhibit clear evidence of assimilation of Archean crust, such as their anomalously low ε_{Nd} (from -16 to -11 at 180 Ma; Fig. 10d) and high Th/Nb (Luttinen & Furnes, 2000; Heinonen et al., 2016). They are characterized by typical tholeiitic low-pressure phenocryst assemblages consisting of varying amounts of plagioclase, clinopyroxene, and olivine, but some of the most primitive samples also contain orthopyroxene phenocrysts.

Before the introduction of MCS, the evolution of the parental magmas of these flood basalts was not well constrained. Although there was evidence of fractional crystallization and assimilation, it was unclear how these processes were linked and what the associated PT-conditions were throughout the evolution of the magma series. MCS modeling revealed that neither FC nor AFC at constant pressure could explain the mineral, major element, trace element, and isotopic composition of the lavas (MCS-AFC model at 500 MPa shown in Fig. 10). The crystallization of orthopyroxene required a pressure of at least 300 MPa (depth of ~10 km), but the Al_2O_3 inflection point at ~7 wt.% of MgO (i.e. beginning of plagioclase fractionation) was not produced with FC or AFC at such high pressures. The best fit was attained with a two-stage model, where the parental magmas first fractionated olivine and orthopyroxene and variably assimilated Archean wallrock at higher pressures (~300–700 MPa), and then fractionated plagioclase, clinopyroxene, and olivine at lower pressures without notable assimilation ($\leq$ 100 MPa). Note that an early stage of AFC is required to explain the full range of trace element ratios (e.g., Zr/Y; Fig. 10c) and radiogenic isotope compositions (Fig. 10d) in the lavas. The presented model is in agreement with thermophysical considerations: assimilation is more likely in magmas either pooled in or slowly moving through deep hotter crust compared to rapid rise of magma through a shallower dike and sill network that is embedded in colder wallrock (Heinonen et al., 2019).

The presented example case provides a strong case of how understanding of igneous petrology benefits from the use of thermodynamically constrained phase equilibria in modeling assimilation and crystallization processes. It could not have been modeled by binary mixing, AFC_{DP}, or EC-AχFC, but requires an internally consistent solution for phase equilibria and major element, trace element, and isotopic compositions that is provided by MCS. An additional example of MCS revealing the effect of recharge and assimilation processes in the geochemical evolution of primitive oceanic island magmas (Kerguelen) is given in Borisova et al. (2017).

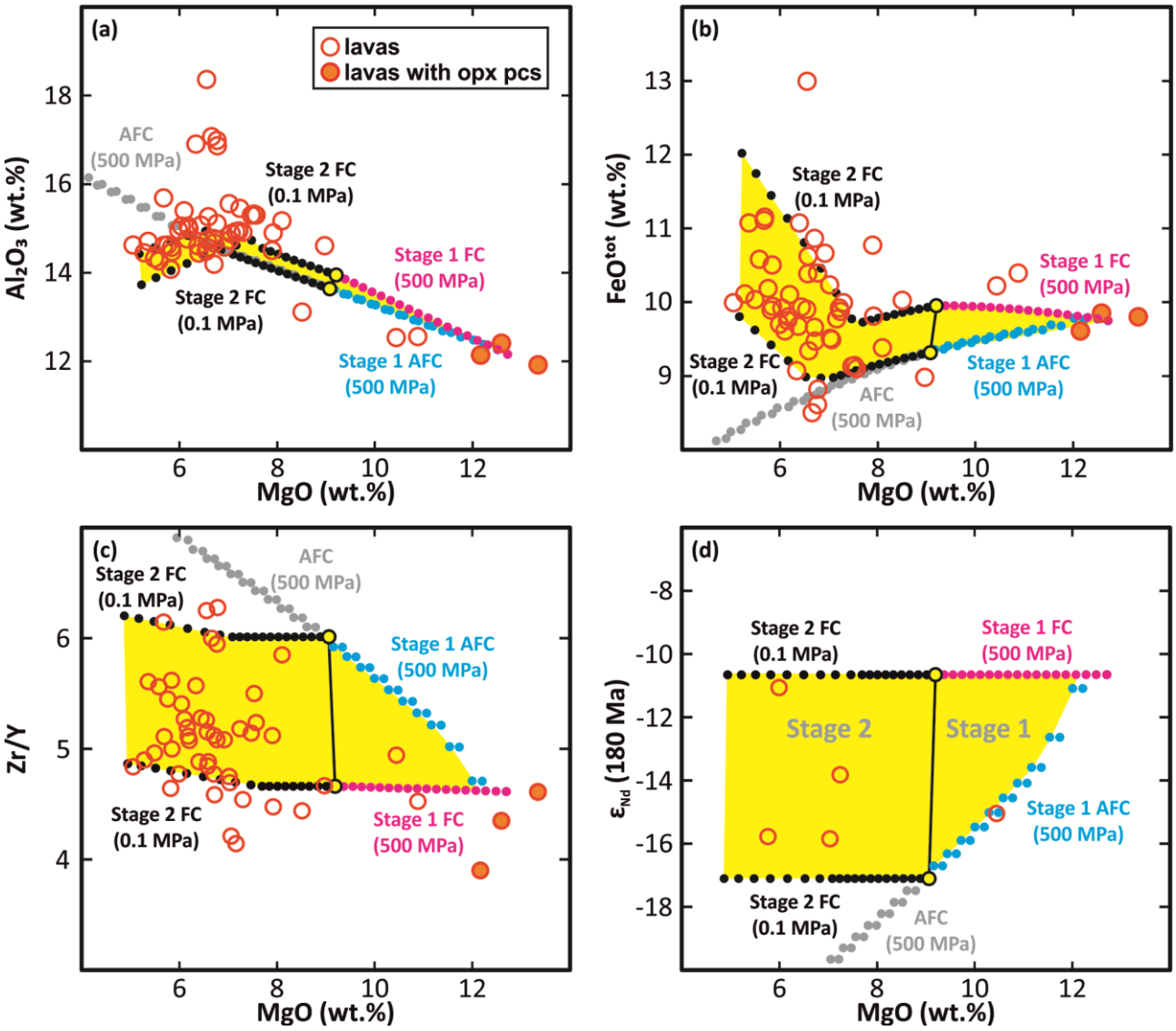

Figure 10. MCS modeling of Antarctic continental flood basalts (~180 Ma Karoo LIP; low-ε_{Nd} CT1 magma type of Luttinen & Furnes, 2000). Primitive lava samples with orthopyroxene phenocrysts are highlighted. Stage 1 is represented by FC and AFC at high pressures (model results at 500 MPa shown here) and is followed by FC during Stage 2 at atmospheric pressure. The yellow field encompasses all possible variations within the end-member Stage 1 + Stage 2 model scenarios. An isobaric (500 MPa) MCS-AFC model shown for reference. For more details, see section 3.6 and Heinonen et al. (2019). Abbreviations: pcs = phenocrysts.

4 Summary

Assimilation, in its simplest form, can be distinguished from other end-member modes of magmatic interaction (hybridization, mingling, and stoping) by the following definition: assimilation is a process in which an initial state (t_0) that includes a system of melt and solid wallrock evolves to a later state (t_n) where the two entities have been completely homogenized into one melt at a given scale. In complex natural systems involving crystallization of the resident melt and melting of the wallrock, this definition can be broadened to describe a process where a mass of magma fully or partially homogenizes with materials derived from wallrock that initially behaves as a solid (i.e., its degree of partial melting is below critical melt fraction).

Our comparison of geochemical assimilation models (binary mixing, AFC_{DP}, EC-AχFC, and MCS) reveals considerable differences in their outcomes using uniform parental melt and wallrock compositions and highlights the value of MCS in understanding thermochemical consequences of assimilation in magmatic systems. We conclude that the use of binary mixing equations in modeling assimilation without any consideration of associated thermodynamics should be avoided. It is very unlikely that any differentiation trend points towards the assimilant composition; therefore, an approach that attempts to define the composition of the assimilant on the basis of hypothetical mixing trends (see, e.g., Pushkar et al., 1971) is inchoate and potentially misleading. On the other end of the modeling spectrum, MCS provides insight into the phase equilibria of crystallization and assimilation. Its use should be favored over AFC_{DP} and EC-AFC models, although in the case of elements that are either highly incompatible or compatible to the resident magma (+ wallrock in the case of EC-AFC models), AFC_{DP} (at low r values) and EC-AFC trends may closely correspond to MCS trends (Fig. 7c). Nevertheless, even in such cases the amount of assimilation indicated by AFC_{DP} or EC-AFC models can be considerably different from that of MCS and likely not be as closely representative of the natural system because of lack of complete (AFC_{DP}) or detailed (EC-AFC) thermodynamic control.

A presented example of MCS applied to a natural system manifests its capabilities by revealing a multi-stage evolution of a continental flood basalt magma system in which the magma system is best modeled by AFC and FC processes that occur at different crustal depths. Finally, we note that the influence of assimilation is always element-specific and dependent on the relative concentrations of different elements in the evolving magma and wallrock and the mass contributions of each of these to the contaminated system. Therefore, if a researcher considers assimilation important, the mass effect should always be specified with respect to what element (or other feature) this importance is defined. MCS is a modeling tool that helps to address this issue.

Acknowledgements

We are grateful to the volume editors for the invitation to contribute. We are grateful to Koshi Nishimura, an anonymous reviewer, and volume editor Christoph Beier for very valuable and balanced commentary that significantly improved the manuscript. This contribution has benefited from the funding by the Academy of Finland (Grant Nos. 295129 and 306962) and the Doctoral school in natural sciences, University of Helsinki. FJS acknowledges continual support from the US National Science Foundation and the US Department of Energy throughout the past four and a half decades.

References

Allègre, C. J., & Minster, J. F. (1978). Quantitative models of trace element behavior in magmatic processes. *Earth and Planetary Science Letters*, 38(1), 1–25. https://doi.org/10.1016/0012-821X(78)90123-1

Ariskin, A. A., Frenkel, M. Y., Barmina, G. S., & Nielsen, R. L. (1993). Comagmat: a Fortran program to model magma differentiation processes. *Computers & Geosciences*, 19(8), 1155–1170. https://doi.org/10.1016/0098-3004(93)90020-6

Arzi, A. A. (1978). Critical phenomena in the rheology of partially melted rocks. *Tectonophysics*, 44(1), 173–184. https://doi.org/10.1016/0040-1951(78)90069-0

Asrat, A., Gleizes, G., Barbey, P., & Ayalew, D. (2003). Magma emplacement and mafic–felsic magma hybridization: structural evidence from the Pan-African Negash pluton, Northern Ethiopia. *Journal of Structural Geology*, 25(9), 1451–1469. https://doi.org/10.1016/S0191-8141(02)00182-7

Beard, J. S., Ragland, P. C., & Crawford, M. L. (2005). Reactive bulk assimilation: A model for crust-mantle mixing in silicic magmas. *Geology*, 33(8), 681–684. https://doi.org/10.1130/G21470AR.1

Bell, K., & Powell, J. L. (1969). Strontium isotopic studies of alkalic rocks: The potassium-rich lavas of the Birunga and Toro-Ankole regions, East and Central Equatorial Africa. *Journal of Petrology*, 10(3), 536–572. https://doi.org/10.1093/petrology/10.3.536

Benkó, Z., Mogessie, A., Molnár, F., Severson, M. J., Hauck, S. A., & Raič, S. (2015). Partial melting processes and Cu-Ni-PGE mineralization in the footwall of the South Kawishiwi Intrusion at the Spruce Road Deposit, Duluth Complex, Minnesota. *Economic Geology*, 110(5), 1269. https://doi.org/10.2113/econgeo.110.5.1269

Bohrson, W. A., & Spera, F. J. (2001). Energy-constrained open-system magmatic processes II: Application of energy-constrained assimilation-fractional crystallization (EC-AFC) model to magmatic systems. *Journal of Petrology*, 42(5), 1019–1041. https://doi.org/10.1093/petrology/42.5.1019

Bohrson, W. A., & Spera, F. J. (2003). Energy-constrained open-system magmatic processes IV: Geochemical, thermal and mass consequences of energy-constrained recharge, assimilation and fractional crystallization (EC-RAFC). *Geochemistry, Geophysics, Geosystems*, 4(2), 8002. https://doi.org/10.1029/2002GC000316

Bohrson, W. A., & Spera, F. J. (2007). Energy-Constrained Recharge, Assimilation, and Fractional Crystallization (EC-RAχFC): A Visual Basic computer code for calculating trace element and isotope variations of open-system magmatic systems. *Geochemistry, Geophysics, Geosystems*, 8(11), Q11003. https://doi.org/10.1029/2007GC001781

Bohrson, W. A., Spera, F. J., Ghiorso, M. S., Brown, G. A., Creamer, J. B., & Mayfield, A. (2014). Thermodynamic model for energy-constrained open-system evolution of crustal magma bodies undergoing simultaneous recharge, assimilation and crystallization: The Magma Chamber Simulator. *Journal of Petrology*, 55(9), 1685–1717. https://doi.org/10.1093/petrology/egu036

Bohrson, W. A., Spera F. J., Heinonen, J. S., Brown, G. A., Scruggs, M. A., Adams, J. V., Takach, M., Zeff, G., & Suikkanen, E. (2020). Diagnosing open-system magmatic processes using the Magma Chamber Simulator (MCS): part I - major elements and phase equilibria. *Contributions to Mineralogy and Petrology*, 175(11), 104. https://doi.org/10.1007/s00410-020-01722-z

Borisova, A. Y., Bohrson, W. A., & Grégoire, M. (2017). Origin of primitive ocean island basalts by crustal gabbro assimilation and multiple recharge of plume-derived melts. *Geochemistry, Geophysics, Geosystems*, 18(7), 2701–2716. https://doi.org/10.1002/2017GC006986

Borisova, A. Y., Martel, C., Gouy, S., Pratomo, I., Sumarti, S., Toutain, J., et al. (2013). Highly explosive 2010 Merapi eruption: Evidence for shallow-level crustal assimilation and hybrid fluid. *Journal of Volcanology and Geothermal Research*, 261, 193–208. https://doi.org/10.1016/j.jvolgeores.2012.11.002

Bowen, N. L. (1915a). The Later Stages of the Evolution of the Igneous Rocks. *The Journal of Geology*, 23(S8), 1–91. https://doi.org/10.1086/622298

Bowen, N. L. (1915b). The crystallization of haplobasaltic, haplodioritic, and related magmas. *American Journal of Science*, s4-40(236), 161–185. https://doi.org/10.2475/ajs.s4-40.236.161

Bowen, N. L. (1915c). Crystallization-differentiation in silicate liquids. *American Journal of Science*, s4-39(230), 175–191. https://doi.org/10.2475/ajs.s4-39.230.175

Bowen, N. L. (1928). *The evolution of igneous rocks*. New York, United States: Dover Publications.

Brandon, A. D. (1989). Constraints on magma genesis behind the Neogene Cascade Arc: Evidence from major and trace element variation of high-alumina and tholeiitic volcanics of the Bear Creek Area. *Journal of Geophysical Research: Solid Earth*, 94(B6), 7775–7798. https://doi.org/10.1029/JB094iB06p07775

Bunsen, R. W. (1851). Über die prozesse der vulkanischen Gesteinsbildungen Islands. *Annotations of Physical Chemistry*, 83, 197–272.

Burda, J., Gawęda, A., & Klötzli, U. (2011). Magma hybridization in the Western Tatra Mts. granitoid intrusion (S-Poland, Western Carpathians). *Mineralogy and Petrology*, 103(1), 19–36. https://doi.org/10.1007/s00710-011-0150-1

Carlson, R. W. (1991). Physical and chemical evidence on the cause and source characteristics of flood basalt volcanism. *Australian Journal of Earth Sciences*, 38(5), 525–544.

Carmichael, I. S. E., Nicholls, J., Spera, F. J., Wood, B. J., Nelson, S. A., Bailey, D. K., et al. (1977). High-temperature properties of silicate liquids: Applications to the equilibration and ascent of basic magma [and discussion]. *Philosophical Transactions of the Royal Society of London.Series A: Mathematical and Physical Sciences*, 286(1336), 373–431.

Carter, S. R., Evensen, N. M., Hamilton, P. J., & O'Nions, R. K. (1978). Neodymium and strontium isotope evidence for crustal contamination of continental volcanics. *Science*, 202(4369), 743–747. https://doi.org/10.1126/science.202.4369.743

Clemens, J. D., & Stevens, G. (2016). Melt segregation and magma interactions during crustal melting: Breaking out of the matrix. *Earth-Science Reviews*, 160, 333–349. https://doi.org/10.1016/j.earscirev.2016.07.012

Cucciniello, C., Langone, A., Melluso, L., Morra, V., Mahoney, J. J., Meisel, T., & Tiepolo, M. (2010). U-Pb ages, Pb-Os isotope ratios, and platinum-group element (PGE) composition of the West-Central Madagascar Flood Basalt Province. *The Journal of Geology*, 118(5), 523–541. https://doi.org/10.1086/655012

Daly, R. A. (1905). The secondary origin of certain granites. *American Journal of Science*, s4-20(117), 185–216. https://doi.org/10.2475/ajs.s4-20.117.185

Daly, R. A. (1910). Origin of the alkaline rocks. *Geological Society of America Bulletin*, 21(1), 87–118. https://doi.org/10.1130/GSAB-21-87

Danckwerts, P. V. (1952). The definition and measurement of some characteristics of mixtures. *Applied Scientific Research: Section A*, 3(4), 279–296. https://doi.org/10.1007/BF03184936

Danckwerts, P. V. (1953). Theory of mixtures and mixing. *Research (London)*, 6, 355–361.

DePaolo, D. J. (1981). Trace element and isotopic effects of combined wallrock assimilation and fractional crystallization. *Earth and Planetary Science Letters*, 53(2), 189–202. https://doi.org/10.1016/0012-821x(81)90153-9

Depaolo, D. J. (1985). Isotopic studies of processes in mafic magma chambers: I. The Kiglapait intrusion, Labrador. *Journal of Petrology*, 26(4), 925-951. https://doi.org/10.1093/petrology/26.4.925

Farner, M. J., Lee, C. A., & Putirka, K. D. (2014). Mafic–felsic magma mixing limited by reactive processes: A case study of biotite-rich rinds on mafic enclaves. *Earth and Planetary Science Letters*, 393, 49–59. https://doi.org/10.1016/j.epsl.2014.02.040

Faure, G., Bowman, J. R., Elliot, D. H., & Jones, L. M. (1974). Strontium isotope composition and petrogenesis of the Kirkpatrick Basalt, Queen Alexandra Range, Antarctica. *Contributions to Mineralogy and Petrology*, 3(3), 153–169. https://doi.org/10.1007/bf00383353

Fenner, C. N. (1926). The Katmai Magmatic Province. *The Journal of Geology*, 34(7), 673–772.

Fred, R., Heinonen, A., & Heikkilä, P. (2019). Tracing the styles of mafic-felsic magma interaction: A case study from the Ahvenisto igneous complex, Finland. *Bulletin of the Geological Society of Finland*, 91(1), 5–33.

Gale, A., Dalton, C. A., Langmuir, C. H., Su, Y., & Schilling, J. (2013). The mean composition of ocean ridge basalts. *Geochemistry, Geophysics, Geosystems*, 14(3), 489–518. https://doi.org/10.1029/2012GC004334

Gardner, M. F., Troll, V. R., Gamble, J. A., Gertisser, R., Hart, G. L., Ellam, R. M., et al. (2013). Crustal differentiation processes at Krakatau volcano, Indonesia. *Journal of Petrology*, 54(1), 149–182. https://doi.org/10.1093/petrology/egs066

Gary, M., McAfee, R., & Wolf, C. L. (Eds.). (1972). *Glossary of Geology*. Washington DC, United States: American Geological Institute.

Ghiorso, M. S. (1985). Chemical mass transfer in magmatic processes; 1, Thermodynamic relations and numerical algorithms. *Contributions to Mineralogy and Petrology*, 90(2–3), 107–120. https://doi.org/10.1007/BF00378254

Ghiorso, M.S., & Gualda, G.A.R. (2015). An H_2O–CO_2 mixed fluid saturation model compatible with rhyolite-MELTS. *Contributions to Mineralogy and Petrology*, 169(6), 53. https://doi.org/10.1007/s00410-015-1141-8

Ghiorso, M., & Kelemen, P. (1987). Evaluating reaction stoichiometry in magmatic systems evolving under generalized thermodynamic constraints: examples comparing isothermal and isenthalpic assimilation. In B. O. Mysen (Ed.), *Magmatic Processes: Physicochemical Principles, The Geochemical Society, Special Publication* (Vol. 1, pp. 319–336).

Ghiorso, M. S., & Sack, R. O. (1995). Chemical mass transfer in magmatic processes IV. A revised and internally consistent thermodynamic model for the interpolation and extrapolation of liquid-solid equilibria in magmatic systems at elevated temperatures and pressures. *Contributions to Mineralogy and Petrology*, 119(2–3), 197–212. https://doi.org/10.1007/bf00307281

Ghiorso, M. S., Hirschmann, M. M., Reiners, P. W., & Kress III, V. C. (2002). The pMELTS: A revision of MELTS for improved calculation of phase relations and major element partitioning related to partial melting of the mantle to 3 GPa. *Geochemistry, Geophysics, Geosystems*, 3(5), 1–35. https://doi.org/10.1029/2001GC000217

Goldstein, S. J., & Jacobsen, S. B. (1987). The Nd and Sr isotopic systematics of river-water dissolved material: Implications for the sources of Nd and Sr in seawater. *Chemical Geology*, 66(3), 245–272. https://doi.org/10.1016/0168-9622(87)90045-5

Goodrich, C. A., & Patchett, P. J. (1991). Nd and Sr isotope chemistry of metallic iron-bearing, sediment-contaminated Tertiary volcanics from Disko Island, Greenland. *Lithos*, 27(1), 13–27. https://doi.org/10.1016/0024-4937(91)90017-F

Grove, T. L., Kinzler, R. J., Baker, M. B., Donnelly-Nolan, J., & Lesher, C. E. (1988). Assimilation of granite by basaltic magma at Burnt Lava flow, Medicine Lake volcano, northern California: Decoupling of heat and mass transfer. *Contributions to Mineralogy and Petrology*, 99(3), 320–343. https://doi.org/10.1007/BF00375365

Gualda, G. A. R., Ghiorso, M. S., Lemons, R. V., & Carley, T. L. (2012). Rhyolite-MELTS: a Modified Calibration of MELTS Optimized for Silica-rich, Fluid-bearing Magmatic Systems. *Journal of Petrology*, 53(5), 875–890. https://doi.org/10.1093/petrology/egr080

Günther, T., Haase, K. M., Klemd, R., & Teschner, C. (2018). Mantle sources and magma evolution of the Rooiberg lavas, Bushveld Large Igneous Province, South Africa. *Contributions to Mineralogy and Petrology*, 173(6), 51. https://doi.org/10.1007/s00410-018-1477-y

Handley, H. K., Reagan, M., Gertisser, R., Preece, K., Berlo, K., McGee, L. E., Barclay, J., & Herd, R. (2018). Timescales of magma ascent and degassing and the role of crustal assimilation at Merapi volcano (2006–2010), Indonesia: Constraints from uranium-series and radiogenic isotopic compositions. *Geochimica et Cosmochimica Acta*, 222, 34–52. https://doi.org/10.1016/j.gca.2017.10.015

Hansen, H., & Nielsen, T. F. D. (1999). Crustal contamination in Palaeogene East Greenland flood basalts: plumbing system evolution during continental rifting. *Chemical Geology*, 157(1–2), 89–118. https://doi.org/10.1016/S0009-2541(98)00196-X

Hayes, B., Bédard, J. H., Hryciuk, M., Wing, B., Nabelek, P., MacDonald, W. D., & Lissenberg, C. J. (2015). Sulfide Immiscibility Induced by Wall-Rock Assimilation in a Fault-Guided Basaltic Feeder System, Franklin Large Igneous Province, Victoria Island (Arctic Canada). *Economic Geology*, 110(7), 1697–1717. https://doi.org/10.2113/econgeo.110.7.1697

Heinonen, J. S., Luttinen, A. V., & Bohrson, W. A. (2016). Enriched continental flood basalts from depleted mantle melts: modeling the lithospheric contamination of Karoo lavas from Antarctica. *Contributions to Mineralogy and Petrology*, 171(1), 9. https://doi.org/10.1007/s00410-015-1214-8

Heinonen, J.S., Luttinen, A.V., Spera, F.J., & Bohrson, W.A. (2019). Deep open storage and shallow closed transport system for a continental flood basalt sequence revealed with Magma Chamber Simulator. *Contributions to Mineralogy and Petrology*, 174(11), 87. https://doi.org/10.1007/s00410-019-1624-0

Heinonen, J. S., Bohrson, W. A., Spera F. J., Brown, G. A., Scruggs, M. A., & Adams, J. V. (2020). Diagnosing open-system magmatic processes using the Magma Chamber Simulator (MCS): part II - trace elements and isotopes. *Contributions to Mineralogy and Petrology*, 175(11), 105. https://doi.org/10.1007/s00410-020-01718-9

Hersum, T. G., Marsh, B. D., & Simon, A. C. (2007). Contact partial melting of granitic country rock, melt segregation, and re-injection as dikes into Ferrar dolerite sills, McMurdo Dry Valleys, Antarctica. *Journal of Petrology*, 48(11), 2125–2148. https://doi.org/10.1093/petrology/egm054

Huppert, H. E., Stephen, R., & Sparks, J. (1985). Cooling and contamination of mafic and ultramafic magmas during ascent through continental crust. *Earth and Planetary Science Letters*, 74(4), 371–386. https://doi.org/10.1016/S0012-821X(85)80009-1

Iacono-Marziano, G., Ferraina, C., Gaillard, F., Di Carlo, I., & Arndt, N. T. (2017). Assimilation of sulfate and carbonaceous rocks: Experimental study, thermodynamic modeling and application to the Noril'sk-Talnakh region (Russia). *Ore Geology Reviews*, 90, 399–413. https://doi.org/10.1016/j.oregeorev.2017.04.027

Jennings, E. S., Gibson, S. A., Maclennan, J., & Heinonen, J. S. (2017). Deep mixing of mantle melts beneath continental flood basalt provinces: Constraints from olivine-hosted melt inclusions in primitive magmas. *Geochimica et Cosmochimica Acta*, 196, 36–57. https://doi.org/10.1016/j.gca.2016.09.015

Johnson, T. E., Gibson, R. L., Brown, M., Buick, I. S., & Cartwright, I. (2003). Partial melting of metapelitic rocks beneath the Bushveld Complex, South Africa. *Journal of Petrology*, 44(5), 789–813. https://doi.org/10.1093/petrology/44.5.789

Jourdan, F., Bertrand, H., Schaerer, U., Blichert-Toft, J., Féraud, G., & Kampunzu, A. B. (2007). Major and trace element and Sr, Nd, Hf, and Pb isotope compositions of the Karoo large igneous province, Botswana-Zimbabwe:

lithosphere vs mantle plume contribution. *Journal of Petrology*, 48(6), 1043–1077. https://doi.org/10.1093/petrology/egm010

Jung, S., Pfänder, J. A., Brauns, M., & Maas, R. (2011). Crustal contamination and mantle source characteristics in continental intra-plate volcanic rocks: Pb, Hf and Os isotopes from central European volcanic province basalts. *Geochimica et Cosmochimica Acta*, 75(10), 2664–2683. https://doi.org/10.1016/j.gca.2011.02.017

Langmuir, C. H., Vocke, R. D., Hanson, G. N., & Hart, S. R. (1978). A general mixing equation with applications to Icelandic basalts. *Earth and Planetary Science Letters*, 37(3), 380–392. https://doi.org/https://doi.org/10.1016/0012-821X(78)90053-5

Larsen, L. M., & Pedersen, A. K. (2009). Petrology of the Paleocene Picrites and Flood Basalts on Disko and Nuussuaq, West Greenland. *Journal of Petrology*, 50(9), 1667–1711. https://doi.org/10.1093/petrology/egp048

Lightfoot, P. C., Hawkesworth, C. J., Hergt, J. M., Naldrett, A. J., Gorbachev, N. S., Fedorenko, V. A., & Doherty, W. (1993). Remobilisation of the continental lithosphere by a mantle plume: major-, trace-element, and Sr-, Nd-, and Pb-isotope evidence from picritic and tholeiitic lavas of the Noril'sk District, Siberian Trap, Russia. *Contributions to Mineralogy and Petrology*, 114(2), 171–188. https://doi.org/10.1007/BF00307754

Luttinen, A. V., & Furnes, H. (2000). Flood basalts of Vestfjella: Jurassic magmatism across an Archaean-Proterozoic lithospheric boundary in Dronning Maud Land, Antarctica. *Journal of Petrology*, 41(8), 1271–1305. https://doi.org/10.1093/petrology/41.8.1271

Mariga, J., Ripley, E. M., & Li, C. (2006). Petrologic evolution of gneissic xenoliths in the Voisey's Bay Intrusion, Labrador, Canada: Mineralogy, reactions, partial melting, and mechanisms of mass transfer. *Geochemistry, Geophysics, Geosystems*, 7(5), Q05013. https://doi.org/10.1029/2005GC001184

McBirney, A. R. (1979). Effects of assimilation. In H. S. Yoder (Ed.), *Evolution of the Igneous Rocks: Fiftieth Anniversary Perspectives* (pp. 307–338). Princeton NJ, United States: Princeton University Press.

Metcalf, R. V., Smith, E. I., Walker, J. D., Reed, R. C., & Gonzales, D. A. (1995). Isotopic Disequilibrium among Commingled Hybrid Magmas: Evidence for a Two-Stage Magma Mixing-Commingling Process in the Mt. Perkins Pluton, Arizona. *The Journal of Geology*, 103(5), 509–527. https://doi.org/10.1086/629773

Molzahn, M., Reisberg, L., & Wörner, G. (1996). Os, Sr, Nd, Pb, O isotope and trace element data from the Ferrar flood basalts, Antarctica: evidence for an enriched subcontinental lithospheric source. *Earth and Planetary Science Letters*, 144(3–4), 529–545. https://doi.org/10.1016/S0012-821X(96)00178-1

Moore, N.E., Grunder, A.L., & Bohrson, W.A. (2018). The three-stage petrochemical evolution of the Steens Basalt (southeast Oregon, USA) compared to large igneous provinces and layered mafic Intrusions. *Geosphere*, 14(6), 2505–2532. https://doi.org/10.1130/GES01665.1

Neuendorf, K. K. E., Mehl, J. P., & Jackson, J. A. (Eds.). (2005). *Glossary of Geology*, 5th Edition. Alexandria, Virginia, United States: American Geological Institute.

Nicholls, J., & Stout,M.,Z. (1982). Heat effects of assimilation, crystallization, and vesiculation in magmas. *Contributions to Mineralogy and Petrology*, 81(4), 328–339. https://doi.org/10.1007/bf00371687

O'Hara, M. J. (1977). Geochemical evolution during fractional crystallisation of a periodically refilled magma chamber. *Nature*, 266(5602), 503–507. https://doi.org/10.1038/266503a0

Oldenburg, C. M., Spera, F. J., Yuen, D. A., & Sewell, G. (1989). Dynamic mixing in magma bodies: Theory, simulations, and implications. *Journal of Geophysical Research: Solid Earth*, 94(B7), 9215–9236. https://doi.org/10.1029/JB094iB07p09215

Petrelli, M., Perugini, D., & Poli, G. (2006). Time-scales of hybridisation of magmatic enclaves in regular and chaotic flow fields: petrologic and volcanologic implications. *Bulletin of Volcanology*, 68(3), 285–293. https://doi.org/10.1007/s00445-005-0007-8

Petrelli, M., Perugini, D., & Poli, G. (2011). Transition to chaos and implications for time-scales of magma hybridization during mixing processes in magma chambers. *Lithos*, 125(1), 211–220. https://doi.org/10.1016/j.lithos.2011.02.007

Pushkar, P., McBirney, A. R., & Kudo, A. M. (1971). The isotopic composition of strontium in Central American ignimbrites. *Bulletin Volcanologique*, 35(2), 265–294. https://doi.org/10.1007/BF02596955

Ramos, F. C., & Reid, M. R. (2005). Distinguishing Melting of Heterogeneous Mantle Sources from Crustal Contamination: Insights from Sr Isotopes at the Phenocryst Scale, Pisgah Crater, California. *Journal of Petrology*, 46(5), 999–1012. https://doi.org/10.1093/petrology/egi008

Reiners, P. W., Nelson, B. K., & Ghiorso, M. S. (1995). Assimilation of felsic crust by basaltic magma: Thermal limits and extents of crustal contamination of mantle-derived magmas. *Geology*, 23(6), 563–566. https://doi.org/10.1130/0091-7613(1995)023<0563:AOFCBB>2.3.CO;2

Rudnick, R. L., & Gao,S. (2003). Composition of the continental crust. In R. L. Rudnick (Ed.), *The Crust, Treatise on Geochemistry* (Vol. 3, pp. 1–64). Oxford, United Kingdom: Elsevier-Pergamon. https://doi.org/10.1016/b0-08-043751-6/03016-4

Samalens, N., Barnes, S., & Sawyer, E. W. (2017). The role of black shales as a source of sulfur and semimetals in magmatic nickel-copper deposits: Example from the Partridge River Intrusion, Duluth Complex, Minnesota, USA. *Ore Geology Reviews*, 81, 173–187. https://doi.org/10.1016/j.oregeorev.2016.09.030

Sparks, R. S. J. (1986). The role of crustal contamination in magma evolution through geological time. *Earth and Planetary Science Letters*, 78(2), 211–223. https://doi.org/10.1016/0012-821X(86)90062-2

Sparks, R. S. J., & Marshall, L. A. (1986). Thermal and mechanical constraints on mixing between mafic and silicic magmas. *Journal of Volcanology and Geothermal Research*, 29(1), 99–124. https://doi.org/10.1016/0377-0273(86)90041-7

Spera, F. J., & Bohrson, W. A. (2001). Energy-constrained open-system magmatic processes I: General model and energy-constrained assimilation and fractional crystallization (EC-AFC) formulation. *Journal of Petrology*, 42(5), 999–1018. https://doi.org/10.1093/petrology/42.5.999

Spera, F. J., & Bohrson, W. A. (2002). Energy-constrained open-system magmatic processes 3. Energy-Constrained Recharge, Assimilation, and Fractional Crystallization (EC-RAFC). *Geochemistry, Geophysics, Geosystems*, 3(12), 8001. https://doi.org/10.1029/2002GC000315

Spera, F. J., & Bohrson, W. A. (2004). Open-System Magma Chamber Evolution: an Energy-constrained Geochemical Model Incorporating the Effects of Concurrent Eruption, Recharge, Variable Assimilation and Fractional Crystallization (EC-E′RAχFC). *Journal of Petrology*, 45(12), 2459–2480. https://doi.org/10.1093/petrology/egh072

Spera, F. J., & Bohrson, W. A. (2018). Rejuvenation of crustal magma mush: A tale of multiply nested processes and timescales. *American Journal of Science*, 318(1), 90–140. https://doi.org/10.2475/01.2018.05

Spera, F. J., Bohrson, W. A., Till, C. B., & Ghiorso, M. S. (2007). Partitioning of trace elements among coexisting crystals, melt, and supercritical fluid during isobaric crystallization and melting. *American Mineralogist*, 92(11-12), 1881–1898. https://doi.org/10.2138/am.2007.2326

Spera, F. J., Schmidt, J. S., Bohrson, W. A., & Brown, G. A. (2016). Dynamics and thermodynamics of magma mixing: Insights from a simple exploratory model. *American Mineralogist*, 101(3), 627–643. https://doi.org/10.2138/am-2016-5305

Taylor, H. P. (1980). The effects of assimilation of country rocks by magmas on $^{18}O/^{16}O$ and $^{87}Sr/^{86}Sr$ systematics in igneous rocks. *Earth and Planetary Science Letters*, 47(2), 243–254. https://doi.org/10.1016/0012-821X(80)90040-0

Tegner, C., Robins, B., Reginiussen, H., & Grundvig, S. (1999). Assimilation of crustal xenoliths in a basaltic magma chamber: Sr and Nd isotopic constraints from the Hasvik layered intrusion, Norway. *Journal of Petrology*, 40(3), 363–380. https://doi.org/10.1093/petrology/40.3.363

Thakurta, J., Ripley, E. M., & Li, C. (2008). Geochemical constraints on the origin of sulfide mineralization in the Duke Island Complex, southeastern Alaska. *Geochemistry, Geophysics, Geosystems*, 9(7), Q07003. https://doi.org/10.1029/2008GC001982

Todesco, M., & Spera, F. J. (1992). Stability of a chemically layered upper mantle. *Physics of the Earth and Planetary Interiors*, 71(1), 85–99. https://doi.org/10.1016/0031-9201(92)90031-P

van der Molen, I. & Paterson, M. S. (1979). Experimental deformation of partially-melted granite. *Contributions to Mineralogy and Petrology*, 70(3), 299–318. https://doi.org/10.1007/BF00375359

Vollmer, R. (1976). Rb-Sr and U-Th-Pb systematics of alkaline rocks: the alkaline rocks from Italy. *Geochimica et Cosmochimica Acta*, 40(3), 283–295. https://doi.org/10.1016/0016-7037(76)90205-2

Walker, B.A.Jr., Miller, C.F., Claiborne, L.L., Wooden, J.L., & Miller J.S. (2007). Geology and geochronology of the Spirit Mountain batholith, southern Nevada: Implications for timescales and physical processes of batholith construction. *Journal of Volcanology and Geothermal Research*, 167 (1–4), 239–262. https://doi.org/10.1016/j.jvolgeores.2006.12.008

Wilcox, R. E. (1954). Petrology of Paricutin volcano, Mexico. *Geological Survey Bulletin*, 965(C), 281–353. https://doi.org/10.3133/b965C

Wilcox, R. E. (1999). The Idea of Magma Mixing: History of a Struggle for Acceptance. *The Journal of Geology*, 107(4), 421–432. https://doi.org/10.1086/314357